Emergent properties of a non-physiological computational model of tumour growth

Pan Pantziarka

NEATG is a simple non-physiological tumour growth model which displays emergent properties which are analogous to a number of characteristics common to physical tumour growth. NEATG employs a novel dual-scale evolutionary algorithm which models both cell-autonomous and non-cell autonomous behaviours. The components of the model are outlined briefly, with reference to the core algorithm and data structures. Experimental results are presented which illustrate the behaviour of the model under different evolutionary scenarios, including homeostasis, tumour growth and a number of anti-tumour interventions. In particular the system is used to explore the impact of cytotoxic interventions, (analogous to high-dose chemotherapy), with respect to adaptive responses and evolutionary change. Finally, a number of avenues for further development of the system are discussed.

PeerJ PrePrints | https://doi.org/10.7287/peerj.preprints.1558v1 | CC-BY 4.0 Open Access | rec: 3 Dec 2015, publ: 3 Dec 2015

Emergent Properties of a Non-physiological Computational Model of Tumour Growth

Pan Pantziarka[1, 2]

[1] The George Pantziarka TP53 Trust, London KT1 2JP, UK

[2]Anticancer Fund, Brussels, 1853 Strombeek-Bever, Belgium

Email Address: Pan Pantziarka: anticancer.org.uk@gmail.com

PeerJ PrePrints | https://doi.org/10.7287/peerj.preprints.1558v1 | CC-BY 4.0 Open Access | rec: 3 Dec 2015, publ: 3 Dec 2015

Abstract

NEATG is a simple non-physiological tumour growth model which displays emergent properties which are analogous to a number of characteristics common to physical tumour growth. NEATG employs a novel dual-scale evolutionary algorithm which models both cell-autonomous and non-cell autonomous behaviours. The components of the model are outlined briefly, with reference to the core algorithm and data structures. Experimental results are presented which illustrate the behaviour of the model under different evolutionary scenarios, including homeostasis, tumour growth and a number of anti-tumour interventions. In particular the system is used to explore the impact of cytotoxic interventions, (analogous to high-dose chemotherapy), with respect to adaptive responses and evolutionary change. Finally, a number of avenues for further development of the system are discussed.

Introduction

Tumour growth is a complex process characterised by multi-scale phenomena involving both cancer and non-cancer cell populations. Where once our focus was directed primarily at the activities of the cancer cell populations, often conceptualised as a single homogeneous mass, our increased understanding of cancer biology now incorporates a more nuanced evolutionary or ecological view of cancer growth (Gatenby, Gillies & Brown, 2011; Kareva, 2011). Key elements of this view of cancer as an evolutionary system are a focus on the genetic heterogeneity of tumour cell populations (De Sousa E Melo et al., 2013; Fisher, Pusztai & Swanton, 2013), the importance of the tumour microenvironment and the cross-talk between cancer and non-cancer cell populations (Allen & Louise Jones, 2011; Hanahan & Coussens, 2012; Quail & Joyce, 2013). A concern among some investigators is that in the absence of an evolutionary understanding of population dynamics in cancer, therapeutic interventions may be doomed to failure (Silva & Gatenby, 2010; Tian et al., 2011; Gillies, Verduzco & Gatenby, 2012). In other cases there is interest in understanding the role of the microenvironment in the process of cancer initiation (Pantziarka, 2015) or the metastatic cascade (Psaila et al., 2007; Barcellos-Hoff, Lyden & Wang, 2013).

More fundamentally, there are also competing theoretical views of cancer at the most basic level. The predominant view of cancer – termed the somatic mutation theory (SMT) – is that it is a disease caused, and then driven, by genetic mutations in cells. An alternative view – termed the tissue-organisation field theory (TOFT) – views cancer as a disease caused by tissue dysfunction, development gone astray, with genetic changes not as the drivers but as a consequence of the disease. A number of recent publications outline these competing views of cancer (Baker, 2014; Bizzarri & Cucina, 2014; Sonnenschein et al., 2014).

Computational models can provide ideal platforms for developing conceptual understanding of complex biological systems (Saetzler, Sonnenschein & Soto, 2011; Janes & Lauffenburger, 2013). A range of techniques are available to build software models of cancer growth specifically designed to explore evolutionary or ecological hypotheses at an abstract and non-physiological level, including techniques from evolutionary game theory (Basanta et al., 2008; Krzeslak & Swierniak, 2014) and machine learning (Gerlee, Basanta & Anderson, 2011). NEATG (Non-physiological Evolutionary Algorithm for Tumour Growth) is a simple software model of tumour growth which models cell-to-cell and tissue-level interactions and population

PeerJ PrePrints | https://doi.org/10.7287/peerj.preprints.1558v1 | CC-BY 4.0 Open Access | rec: 3 Dec 2015, publ: 3 Dec 2015

dynamics under different evolutionary scenarios. This paper describes the structure of this model and explores a range of results under different scenarios, in particular there is a focus on results which are pertinent to real cancer growth and which reflect on some of the issues outlined above.

Methods

NEATG is implemented as a hybrid model incorporating elements from both genetic algorithms and cellular automata. It is dual scale, non-deterministic and represents both cell-level and tissue-level behaviour. It is coded in the Java programming language.

Grid or Tissue-Level

The tissue-level is represented as an N x M grid, with each grid element containing a set of modelled cells (which may be malignant or normal). The relative proportion of normal and malignant cells in a grid element determines the state of that grid element. These states are:

$$E = \{\text{Normal, Majority Normal, Majority Malignant, Tumour, Necrotic}\}$$

Transition of a grid element from one state to another takes place at every clock tick and is determined by the proportions of different cell populations within that element, but also by the state of neighbouring grid elements. Grid elements which are in the Tumour state, that is they do not have any normal cells within them, can transition to a Necrotic state if they are surrounded by an extended neighbourhood which consists exclusively of other Tumour grid elements. By default the neighbourhood is a Moore neighbourhood of radius 2 (see Figure 1), though this is a configurable model parameter.

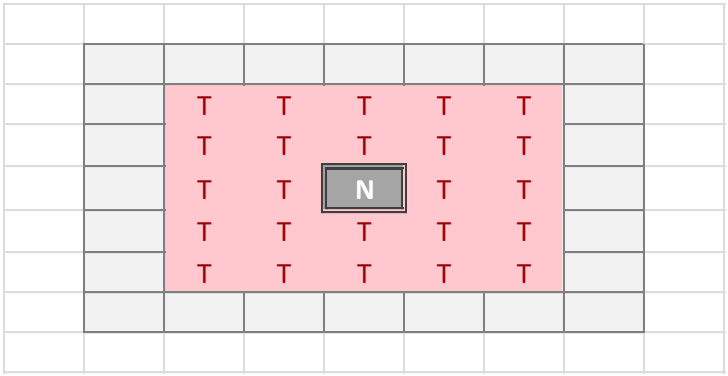

Figure 1 - Moore Neighbourhood of radius 2

Grid elements in the Necrotic state are suspended and do not take part in further computational activity unless the neighbouring grid population changes, in which case the Necrotic state reverts to Tumour.

Each grid element is populated with an initial, optimum population of normal cells. The size of this optimum population is a model parameter that can be varied. The size of the population can vary over time and can increase to a defined maximum value after which cellular competition takes place (as described below).

Each grid element receives as input a Nutrient, represented as an integer value, and a set of Gene Factors, represented as real values. The number of Gene Factors is equal to the number of genes in the cell structure, again this is a model parameter that can vary, but the default number is 3.

PeerJ PrePrints | https://doi.org/10.7287/peerj.preprints.1558v1 | CC-BY 4.0 Open Access | rec: 3 Dec 2015, publ: 3 Dec 2015

The Nutrient score can be loosely interpreted as a combination of oxygen and cellular nutrients (e.g. glucose), while the Gene Factors may be viewed as generic growth factors required for cellular growth and survival.

The grid element has a distribution function to compute the share of Nutrient (*DN*) assigned to each cell in its population of *P* cells based on the relative demand represented by the Nutrient Target values *T*:

$$DN_i = \frac{T_i}{\sum_{p=1}^{P} T_p}$$

Similarly the Gene Factor values which are inputs into each grid element are distributed to each cell according to the transfer function based on the Gene Targets (*G*):

$$DG_i = \frac{G_i}{\sum_{p=1}^{P} G_p}$$

Cell Level

Each cell is a data structure that encodes a Genome and an internal clock. The internal clock, implemented as an integer value, counts down from a maximum value, known as the Lifetime, to zero. When the system is first instantiated each cell is initialised with an internal clock value that is equal to a random integer between the Lifetime and zero. The Genome is a set of N genes, which are defined by a Target and a Tolerance, both represented as real numbers. The Genome and is defined as:

G = {(Target*0*, Gene Tolerance*0*)…(Target*N*, Tolerance*N*)}

The Target is the optimum required level of the corresponding Gene Factor that is supplied by the local grid environment, and the Tolerance defines a band of values on either side of the Target which is considered the healthy range for that gene.

Gene health is therefore defined as a Boolean value:

Health = (Gene Factor < (Gene Target + Gene Tolerance)) & (Gene Factor > (Gene Target – Gene Tolerance))

In addition to flagging health status, Genes are also used as a mechanism for the cell to influence the local grid environment. This is a simple feedback mechanism by which each cell attempts to alter the local environment in order to achieve the level of Gene Factor required for its own optimum health. The expression function is:

$$E = 1 - e^{-(T-F)}$$

Where *T* is the Gene Target value and *F* exogenously supplied Factor.

The actual level of Gene Factor available in each Grid Element is calculated as the sum of the exogenously supplied Factor, which is an input parameter in the model, and the sum of the expression values from each cell in that grid element.

PeerJ PrePrints | https://doi.org/10.7287/peerj.preprints.1558v1 | CC-BY 4.0 Open Access | rec: 3 Dec 2015, publ: 3 Dec 2015

Additional components of the cell are the Lifetime value (the maximum number of clock ticks before cell division takes place), a Nutrient Target and a Nutrient Rate, which represent the demand for nutrient and the metabolic rate at which nutrient is consumed respectively. Nutrient which is not consumed is stored in the Nutrient Store. Each cell also has a Mutation Rate and an Invasion Rate, which are used when cell division is necessitated for Malignant cells.

Cells can exist in a number of states:

$$CS = \{\text{HEALTHY, DIVIDING, APOPTOTIC, TO\_BE\_CLEARED, NECROTIC}\}$$

Note that the cell state of Healthy implies viability, rather than whether or not a cell is Normal or Malignant.

Additionally there are two types of cell in this model, Normal and Malignant. Note that the structure of cells is the same regardless of cell type. However, while the structure is the same the behaviour is type-dependent during cell division.

At every clock tick the health status of the cell is assessed and the cell clock decremented according to the state of health. A healthy cell, that is with adequate Nutrient and Gene Factors, will decrease the cell clock by 1. Each unhealthy gene will also decrement the cell clock by one, whereas a cell that has a value of zero for Nutrient store will have the cell clock set to zero, to indicate that the cell must divide.

All cells undergo a similar cell cycle. A cell starts as Healthy and undergoes a number of iterations (clock ticks) in which nutrient and gene factors are processed, the cell clock decreases at rates that depend on how well the cell is adapted to the local grid environment defined by the available Nutrient and Gene Factors. When the cell clock or nutrient store reaches zero the cell changes state according to the following cycle:

$$\text{Healthy} > \text{Dividing} > \text{Apoptotic} > \text{To Be Cleared}$$

Cells that are flagged as To Be Cleared are removed from the grid element. At each iteration dividing cells undergo cell division during which a new daughter cell is generated and enters the local population in the grid element. When the grid element contains fewer than the maximum supported cells (termed the carrying capacity of the grid element) a new cell is cloned from the dividing cell. In the case of Malignant cells this cloning can also incur a mutation in which one of the elements of the cell can change value, for example the Nutrient Target, a Gene Tolerance value or the cell Lifetime itself may undergo an increase or decrease. Note that the rate of mutation events is controlled by the Mutation Rate, which is itself mutable and can increase or decrease through mutation.

If the grid element is already supporting the maximum number of cells then the cell division process is more complex. In addition to undergoing the chance of mutation, Malignant cells may also undergo a migration event in which the cell moves into a randomly selected adjacent grid element. The rate of such migration events is controlled by the Invasion Rate, which, like the Mutation Rate, is itself mutable. Cells which are not selected for migration are added to the local population. To preserve the carrying capacity of the grid element, all cells are then ranked according to fitness and the least fit cells are removed. This ranked selection algorithm is not biased by cell type, and both Malignant and Normal cells are included in the process.

PeerJ PrePrints | https://doi.org/10.7287/peerj.preprints.1558v1 | CC-BY 4.0 Open Access | rec: 3 Dec 2015, publ: 3 Dec 2015

The fitness function F is defined as:

$$F = \sum_{g=1}^{G} e^{-\left(|T_g - A_g| / T_g\right)}$$

where T is the Gene Target and A is the Gene Factor value for each Gene in the Genome *G*.

The fitness function is designed to penalise cells which are poorly adapted to the local environment.

Evolutionary Strategies

Each iteration the processing of Nutrient and Gene Factors is controlled by a treatment strategy object. This software component enables the NEATG system to model multiple evolutionary strategies, each of which can implement different algorithms in terms of controlling the rate of cellular attrition, ageing and division. For example it is possible to implement a strategy which mimics high-dose chemotherapy and stops dividing cells from successfully completing the replication process. Alternatively a treatment strategy may alter the nutrient supply to mimic starvation or over-feeding.

Treatment strategies can be designed so that they become active at specific time points, either by activation at a specified iteration or a specified level of tumour growth. Once triggered a treatment strategy can remain active until the final iteration or remain active for a specified number of iterations. There is also a default 'do nothing' strategy which remains active for the iterations before and after the 'active' strategy has been triggered.

Run-time Behaviour

The run-time behaviour of NEATG is specified using a scenario file which sets the key parameters which describe both the structure of the grid and the cell populations. Initial parameters include the size of the grid, in terms of width and length, optimum and maximum cell counts for grid elements, the number of iterations or clock-ticks, the active strategy and the trigger point and duration of action. In terms of cell structure the key parameters include the number of genes, the gene structure, the mutation and invasion rates and the lifetime of each cell. Another key input to the system is the structure of the Malignant cell, both in terms of the gene structure but also in terms of the number of malignant cells to insert into the system and at which iteration they should be inserted.

There are numerous logging, statistics and output generation features implemented by the system, and these too are controlled via the scenario file. As the system is non-deterministic and displays considerable variation in behaviour depending on the evolutionary processes of mutation and invasion, an additional scripting mechanism is implemented so that multiple runs can be performed and the data stored together for analysis and reporting.

PeerJ PrePrints | https://doi.org/10.7287/peerj.preprints.1558v1 | CC-BY 4.0 Open Access | rec: 3 Dec 2015, publ: 3 Dec 2015

Results

Homeostasis

Before exploring the results for different tumour growth scenarios it is important to validate the behaviour of the system during homeostatic and non-tumour scenarios. Cells in this scenario should be supplied with target Nutrient and Gene Factor values, ensuring that they are unstressed and in 'good health'. In the absence of tumour cells we would expect that the system will display homeostatic behaviour characterised by regular cellular turn-over as cells age and die, and that cell populations will fluctuate but remain relatively constant.

To represent this scenario a series of experiments were run using a 25 x 25 grid. The optimum cell population for each grid was set at 5, with a population of 10 cells as the maximum carrying capacity. The Nutrient Target used was 10, with a Nutrient Rate of 1. The Nutrient input to each grid element was also set at 10, ensuring that at optimum population level each cell would receive a Nutrient input of 10 / 5 = 2. A genome of three identical genes was used:

$$G = \{(5.0, 1.0), (5.0, 1.0), (5.0, 1.0)\}$$

The Gene Factor supplied to each grid element was set at {25.0, 25.0, 25.0}, to ensure that each cell received the Gene Target value of 5.0.

The system was run five times, with 1000 iterations per run, and the results averaged for this analysis. Given our input parameters for a grid of 625 elements (25 x 25), and an optimum cell density of 5 cells per grid element, we would expect a total cell count of 3125. However, not all of these cells will be healthy, some will be dividing or being cleared. Figure 2 shows the overall population density over time.

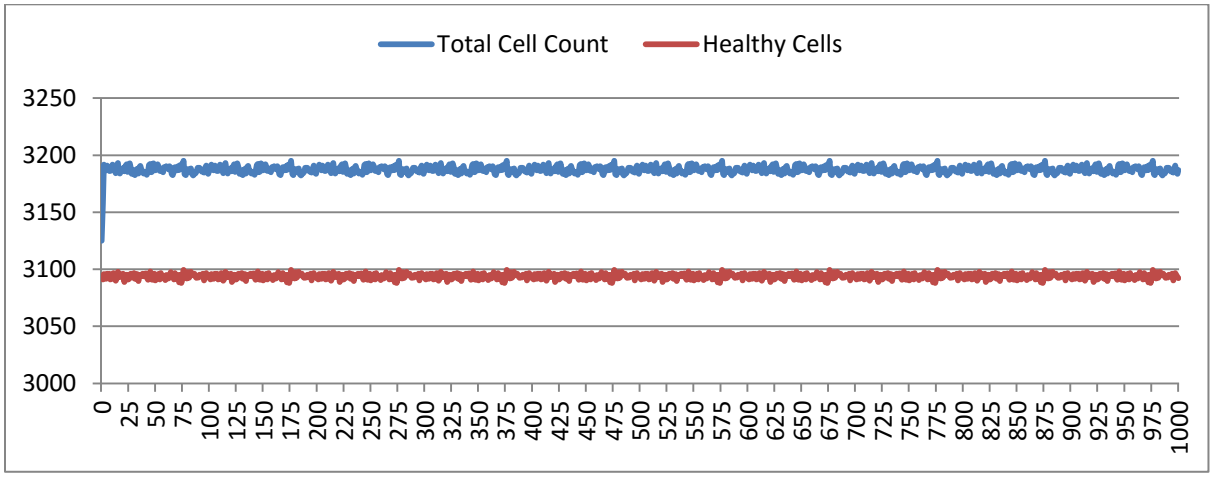

Figure 2 - Total cell count and healthy cell count

We can also see the number of dividing cells over time, as in Figure 3.

PeerJ PrePrints | https://doi.org/10.7287/peerj.preprints.1558v1 | CC-BY 4.0 Open Access | rec: 3 Dec 2015, publ: 3 Dec 2015

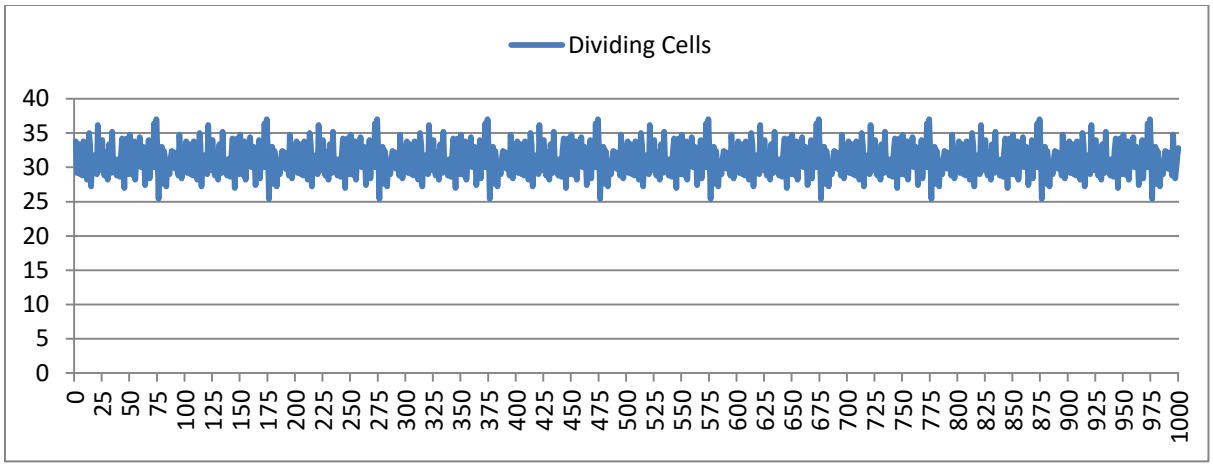

Figure 3 - Number of dividing cells over time

Note that the average number of dividing cells over the 1000 iterations is 31.25. This is as we would expect given that the Lifetime for the cells is 100, so that at any one time 1% of cells is dividing. The total population cell count includes dividing cells and those in the process of being cleared, therefore it is higher than the 3125 we might expect, but clearly it fluctuates around a constant value. The average over the 1000 iterations is 3187.4, which is actually 2% above 3125 – this value represents 1% of cells which are dividing and another 1% of cells which are being cleared during any single iteration.

Finally we can assess the average fitness of the cells, shown in Figure 4, and the average age of the cells, shown in Figure 5.

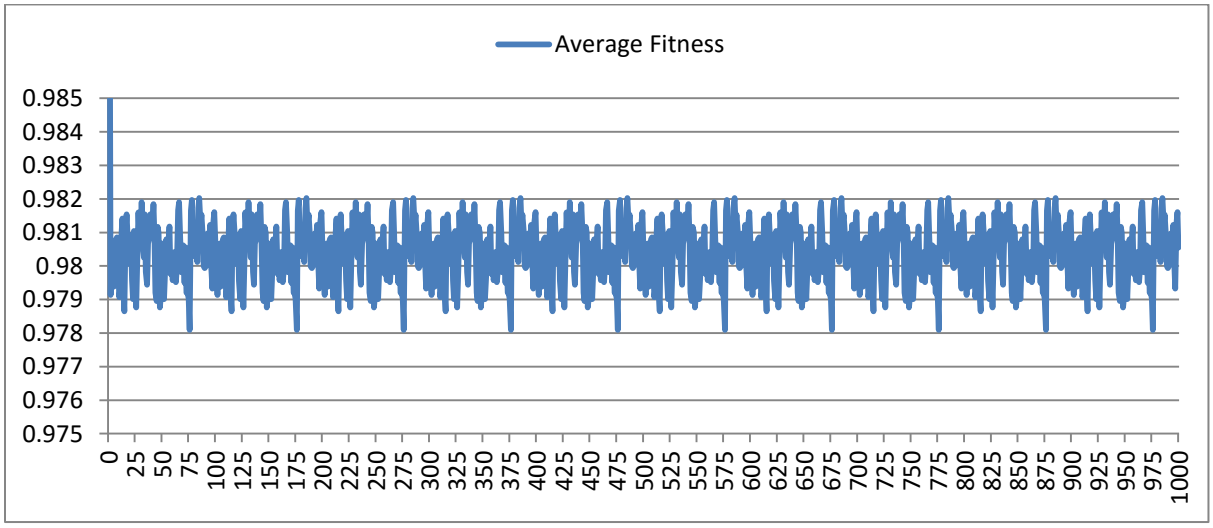

Figure 4 - Average fitness of cells

PeerJ PrePrints | https://doi.org/10.7287/peerj.preprints.1558v1 | CC-BY 4.0 Open Access | rec: 3 Dec 2015, publ: 3 Dec 2015

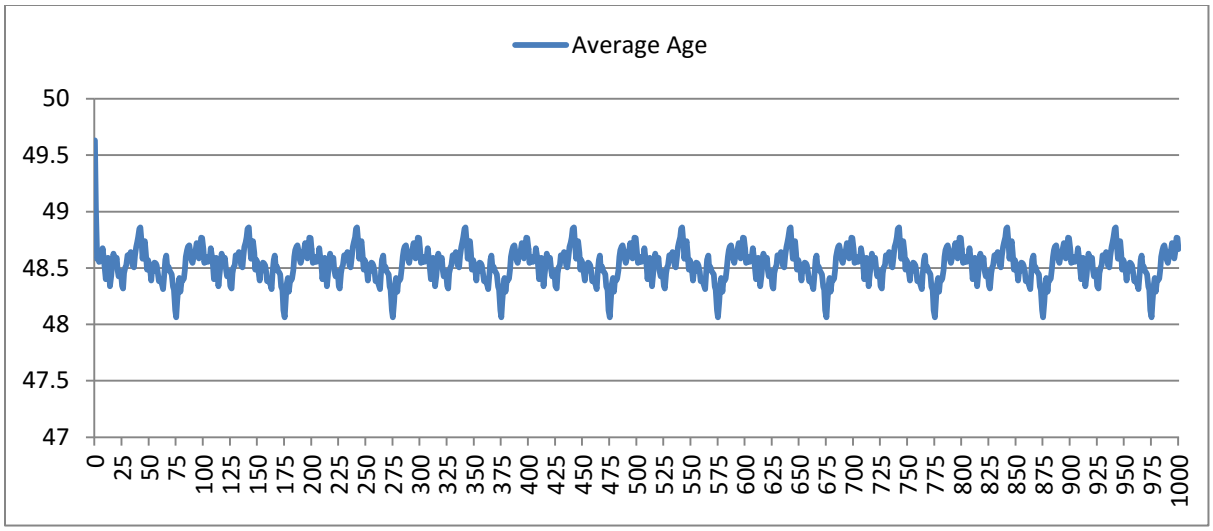

Figure 5 - Average age of cells

Again the values for fitness and age are as we would expect. The average fitness is high, fluctuating just below the maximum possible value of 1.0. And the average age fluctuates just below a value of 50. These latter two figures display more clearly a pronounced periodicity which is also evident in the population density figure. This is due to the random distribution of ages in the initial cell population. In the absence of stress or environmental perturbation the population of cells ages and divides in a uniform manner that preserves that initial distribution of ages in the initial cell population.

Stress Conditions

In the next experiments we assess the behaviour of NEATG when homeostasis is disturbed. In particular we are interested in the responses to changes in Nutrient and Gene Factors as these both have an influence on cell ageing and survival. Again this series of experiments does not include Malignant cells as we are primarily interested in exploring the behaviour of the system in non-tumour scenarios. For both of the following experiments the same basic parameters as in the previous experiment are used. The results shown are the average of 5 runs of the system.

The first stress experiment varies the Nutrient input to each grid element in the range 1 to 15, in integer steps. Given that the Nutrient Rate is set at a value of 1 and the optimum cell population is set to 5, we would expect that if the Nutrient Supply to each grid element falls below a value of 5 each cell in the grid would consume more nutrient than it receives as input and eventually deplete the value in its Nutrient Store (which was set to an initial value of 10). When we look at the number of healthy cells with different Nutrient Supply values we see a decline in cell numbers over time, as shown in Table 1. It is clear that number of healthy cells declines sharply when there is insufficient Nutrient supplied, but that ‘over-feeding’ (any Nutrient Supply value above 5) does not increase cell numbers.

PeerJ PrePrints | https://doi.org/10.7287/peerj.preprints.1558v1 | CC-BY 4.0 Open Access | rec: 3 Dec 2015, publ: 3 Dec 2015

Gen	NS=1	NS=2	NS=3	NS=4	NS=5	NS=6	NS=7	NS=8	NS=9	NS=10	NS=11	NS=12	NS=13	NS=14	NS=15
0	3094	3093	3095	3092	3097	3099	3092	3095	3091	3091	3090	3096	3093	3097	3096
5	2884	2877	2876	2884	3095	3094	3094	3093	3093	3093	3095	3096	3095	3093	3091
10	2600	2593	2601	2636	3098	3096	3092	3099	3094	3094	3091	3097	3097	3098	3093
15	45	2242	2264	2375	3090	3094	3097	3093	3097	3094	3092	3095	3088	3095	3093
20	0	577	1920	2129	3096	3090	3091	3092	3093	3094	3095	3089	3094	3093	3093
25	0	331	778	1906	3095	3097	3089	3093	3091	3095	3093	3086	3091	3095	3094
30	0	379	660	1731	3093	3094	3099	3094	3091	3097	3089	3093	3097	3094	3090
35	0	381	605	1591	3093	3091	3097	3093	3097	3090	3091	3094	3096	3093	3091
40	0	355	598	1455	3097	3094	3093	3096	3094	3096	3101	3094	3093	3094	3095
45	0	373	584	1370	3095	3094	3093	3094	3094	3095	3095	3095	3091	3094	3097
50	0	358	578	1188	3089	3094	3094	3092	3094	3092	3095	3095	3090	3096	3093

Table 1 - Healthy cells for different Nutrient Supply values

The change in the number of Healthy cells is shown more clearly for Nutrient Supply values in the range 1 to 5 in Figure 6.

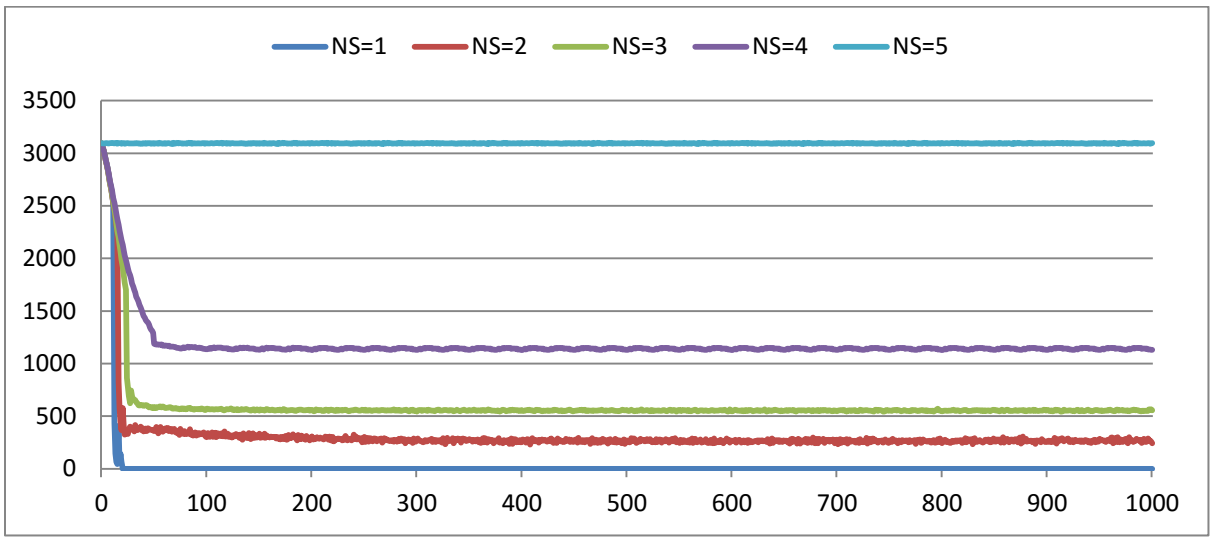

Figure 6 - Change in Healthy Cell count in response to underfeeding

If we look at the change in Fitness in response to different Nutrient Supply values, Table 2, we see a concomitant decrease in over time in the case of 'under feeding' but no additional increase in fitness in response to over-feeding.

PeerJ PrePrints | https://doi.org/10.7287/peerj.preprints.1558v1 | CC-BY 4.0 Open Access | rec: 3 Dec 2015, publ: 3 Dec 2015

Gen	NS=1	NS=2	NS=3	NS=4	NS=5	NS=6	NS=7	NS=8	NS=9	NS=10	NS=11	NS=12	NS=13	NS=14	NS=15
0	0.990	0.990	0.990	0.989	0.991	0.992	0.990	0.990	0.989	0.989	0.989	0.991	0.990	0.991	0.991
10	0.696	0.709	0.700	0.694	0.973	0.974	0.969	0.974	0.969	0.971	0.971	0.970	0.973	0.972	0.968
20	0.000	0.005	0.510	0.468	0.971	0.969	0.970	0.970	0.973	0.972	0.971	0.969	0.971	0.971	0.971
30	0.000	0.000	0.003	0.294	0.970	0.971	0.972	0.971	0.969	0.973	0.969	0.970	0.972	0.967	0.969
40	0.000	0.000	0.000	0.167	0.969	0.971	0.969	0.971	0.970	0.972	0.971	0.971	0.972	0.970	0.970
50	0.000	0.000	0.000	0.021	0.970	0.970	0.971	0.971	0.971	0.968	0.970	0.971	0.969	0.971	0.969
60	0.000	0.000	0.000	0.014	0.970	0.969	0.971	0.970	0.970	0.971	0.969	0.971	0.971	0.970	0.973
70	0.000	0.000	0.000	0.013	0.971	0.971	0.971	0.972	0.971	0.972	0.973	0.968	0.972	0.971	0.969
80	0.000	0.000	0.000	0.013	0.970	0.972	0.969	0.970	0.969	0.971	0.972	0.971	0.971	0.970	0.970
90	0.000	0.000	0.000	0.013	0.971	0.971	0.971	0.969	0.970	0.971	0.971	0.970	0.971	0.970	0.971
100	0.000	0.000	0.000	0.013	0.971	0.971	0.969	0.970	0.969	0.970	0.969	0.971	0.971	0.971	0.972

Table 2- Change in Average Fitness in response to underfeeding

It is clear then that cell populations are sensitive to the supply of Nutrient, and that under-feeding can deplete numbers and in some cases 'starvation' reduces cell numbers to zero. Over-feeding, on the other hand, does not increase cell numbers nor does it increase fitness.

The supply of Gene Factors is the other external input to each grid element. These are analogous to generic growth and survival factors and are used to assess the health or otherwise of each cell in a grid element. As described previously, each Gene is defined as a Target and a Tolerance, and cells are able to 'express' a Gene Factor in order to influence the local environment so that it matches the desired Target value. In this experiment the same parameters are used as before, but the Gene Factor Supply is varied from {0.0, 0.0, 0.0} to {45.0, 45.0, 45.0} by incrementing each element of the by 5.0 for every step. Five runs were completed for each setting and the averages used in the analysis.

In terms of cell numbers the results are shown in Table 3. While there are no significant reductions in cell numbers, it is clear that at the optimal level (Gene Factor Supply = {25.0, 25.0, 25.0}) the number of healthy cells is highest. Figures are shown for the first 100 generations only as there is limited change beyond this point.

Gen	GS=0	GS=5	GS=10	GS=15	GS=20	GS=25	GS=30	GS=35	GS=40	GS=45
0	2998	3001	2998	2998	3010	3095	3002	3001	3009	2993
10	2994	3003	2999	2994	3098	3096	3003	2998	2986	3000
20	2997	3000	2999	3003	3096	3093	2992	2997	2996	3002
30	3005	3001	3008	3007	3092	3094	2990	2993	3002	3002
40	3003	2995	3000	3000	3093	3096	3002	3002	3008	3004
50	2998	3001	2998	2998	3091	3096	3035	3001	3009	2993
60	2994	3003	2999	2994	3089	3092	3002	2998	2986	3000
70	2997	3000	2999	3003	3094	3093	2992	2997	2996	3002
80	3005	3001	3008	3007	3089	3092	2990	2993	3002	3002
90	3003	2995	3000	3000	3090	3095	3001	3002	3008	3004
100	2998	3001	2998	2998	3010	3095	3035	3001	3009	2993

Table 3 - Healthy cell counts vs Gene Factor Supply

PeerJ PrePrints | https://doi.org/10.7287/peerj.preprints.1558v1 | CC-BY 4.0 Open Access | rec: 3 Dec 2015, publ: 3 Dec 2015

If we look at the numbers of dividing cells, a measure of cell turnover, as shown in Table 4, then we can see that there is a pronounced effect.

Gen	GS=0	GS=5	GS=10	GS=15	GS=20	GS=25	GS=30	GS=35	GS=40	GS=45
0	127	124	127	127	115	30	123	124	116	132
10	131	122	126	131	27	29	122	127	139	125
20	128	125	126	122	29	32	133	128	129	123
30	120	124	117	118	33	31	135	132	123	123
40	122	130	125	125	32	29	123	123	117	121
50	127	124	127	127	34	29	90	124	116	132
60	131	122	126	131	36	33	123	127	139	125
70	128	125	126	122	31	32	133	128	129	123
80	120	124	117	118	36	33	135	132	123	123
90	122	130	125	125	35	30	124	123	117	121
100	127	124	127	127	115	30	90	124	116	132

Table 4 - Cell turnover vs Gene Factor Supply

The number of dividing cells at the optimal Gene Factor Supply value is around 1% of the total cell count, whereas for non-optimal Supply values there is an increased rate of cell division. This is as we would expect given that unhealthy genes (i.e. those in which the Gene Factor Supply is outside of the range defined by the Target and Tolerance values) cause an increased rate of cell aging by increasing the rate at which the cell clock is decremented to zero.

In addition to being a factor in the cellular aging process, the Genes are also used in calculations of cell fitness. Cell fitness is used in the rank selection process to identify the least fit cells when the population density in a grid element exceeds the maximum capacity. In this experiment no Malignant cells are present therefore the rank selection procedure is not active; however we can still assess the influence of the Gene Factor Supply on cell fitness. Fitness, which is defined in the range [0, 1], is shown in Figure 7.

PeerJ PrePrints | https://doi.org/10.7287/peerj.preprints.1558v1 | CC-BY 4.0 Open Access | rec: 3 Dec 2015, publ: 3 Dec 2015

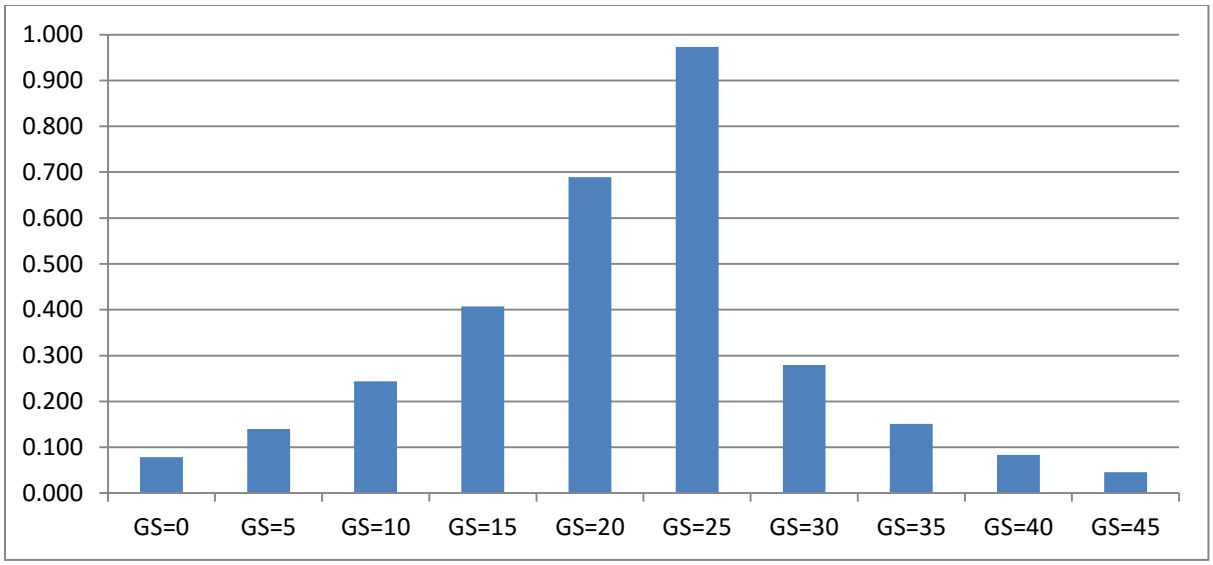

Figure 7 - Average fitness vs Gene Factor Supply

Finally, we have explained that Genes attempt to influence the local environment through expression of Gene Factors. This is a simple feedback mechanism between the cell and its Genes and the exogenous Gene Factor Supply. In this experiment each Gene has been set to the same value (5.0, 1.0), and therefore we can focus on a single Gene, shown in Table 5, to view the change in Gene Expression over time:

Gen	GS=0	GS=5	GS=10	GS=15	GS=20	GS=25	GS=30	GS=35	GS=40	GS=45
0	0.953	0.943	0.911	0.830	0.609	0.000	-1.651	-6.135	-18.375	-51.341
10	0.872	0.850	0.785	0.646	0.422	0.000	-5.375	-16.239	-45.692	-126.673
20	0.871	0.848	0.786	0.649	0.422	0.000	-5.362	-16.379	-45.604	-127.078
30	0.875	0.850	0.787	0.649	0.421	0.000	-5.359	-16.268	-45.982	-126.558
40	0.876	0.845	0.786	0.647	0.421	0.000	-5.364	-16.218	-45.961	-126.482
50	0.874	0.848	0.783	0.647	0.421	0.000	-5.446	-16.393	-46.137	-125.932
60	0.872	0.850	0.785	0.646	0.421	0.000	-5.376	-16.239	-45.692	-126.673
70	0.871	0.848	0.786	0.649	0.422	0.000	-5.362	-16.379	-45.604	-127.078
80	0.875	0.850	0.787	0.649	0.420	0.000	-5.357	-16.268	-45.982	-126.558
90	0.876	0.845	0.786	0.647	0.421	0.000	-5.365	-16.218	-45.961	-126.482
100	0.874	0.848	0.783	0.647	0.417	0.000	-5.446	-16.393	-46.137	-125.932

Table 5 - Gene Expression vs Gene Factor Supply

Note that in optimal conditions cells do not need to exert any influence on the local environment as the Gene Factor Supply matches the Target value. When the supply is deficient, the Gene expression is positive to increase the supply, when the supply is excessive the Gene expression is negative to reduce the supply. The steady state values shown in Table 5 mask a considerably noisy signal, which is more clearly apparent in Figure 8, which shows the change over time for two non-optimal Gene Factor Supply values.

PeerJ PrePrints | https://doi.org/10.7287/peerj.preprints.1558v1 | CC-BY 4.0 Open Access | rec: 3 Dec 2015, publ: 3 Dec 2015

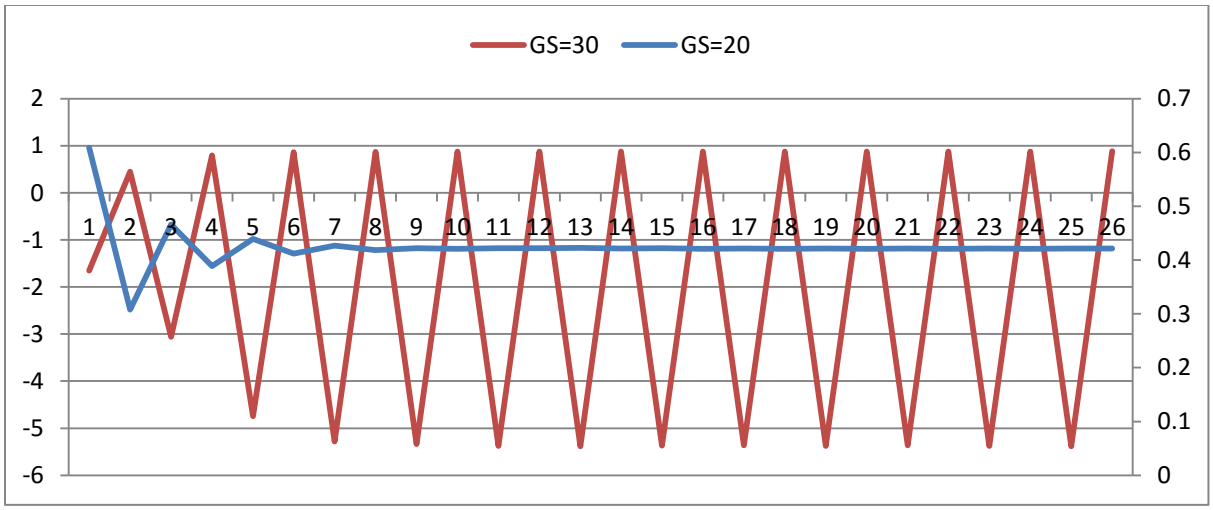

Figure 8 - Gene Expressions vs Gene Factor Supply

The oscillating Gene Expression is the result of each cell trying to correct the local environment to supports its own needs – and we see therefore the resultant fluctuations as cells over- and under-correct in turn.

Tumour Growth – No Treatment

Having established the behaviour of the system under homeostatic and non-tumour stress scenarios, we can now begin to introduce Malignant cells. Initially we will explore the behaviour of NEATG in the absence of any treatment scenarios – we first want to explore the behaviour of Malignant cells and how they model tumour growth.

In this first series of experiments we will continue to use the same parameters as we have for the homeostasis and non-tumour stress experiments, although the iteration period is increased to 2000 to allow greater time for the evolution of appreciable tumour masses. Tumour growth is initiated by the insertion of a single Malignant cell into the grid element in the centre of our 25 x 25 grid. The only difference between this Malignant cell and the Normal cells is that the cell type is set to Malignant, and that it has a mutation rate of 5% and an invasion rate of 10%. These initial values were derived from empirical testing of NEATG and were selected for this first experiment as they yielded consistent tumour growth. In subsequent experiments these values will be varied so that we can see how tumour growth patterns are affected.

The difference between the grid element level and the cell level is apparent when we begin to analyse the results of these experiments. In the non-tumour experiments all grid elements were considered Normal, and analysis looking only at the changes in cell counts was sufficiently informative as regards changes in the system. However, with the introduction of Malignant cells we can view results both in terms of the changes in cell populations across the whole system and also in the evolution of the grid elements themselves.

The results shown are the average of 5 runs of the system.

PeerJ PrePrints | https://doi.org/10.7287/peerj.preprints.1558v1 | CC-BY 4.0 Open Access | rec: 3 Dec 2015, publ: 3 Dec 2015

The change in the global population counts in the Normal and Malignant cells is shown in Figure 9.

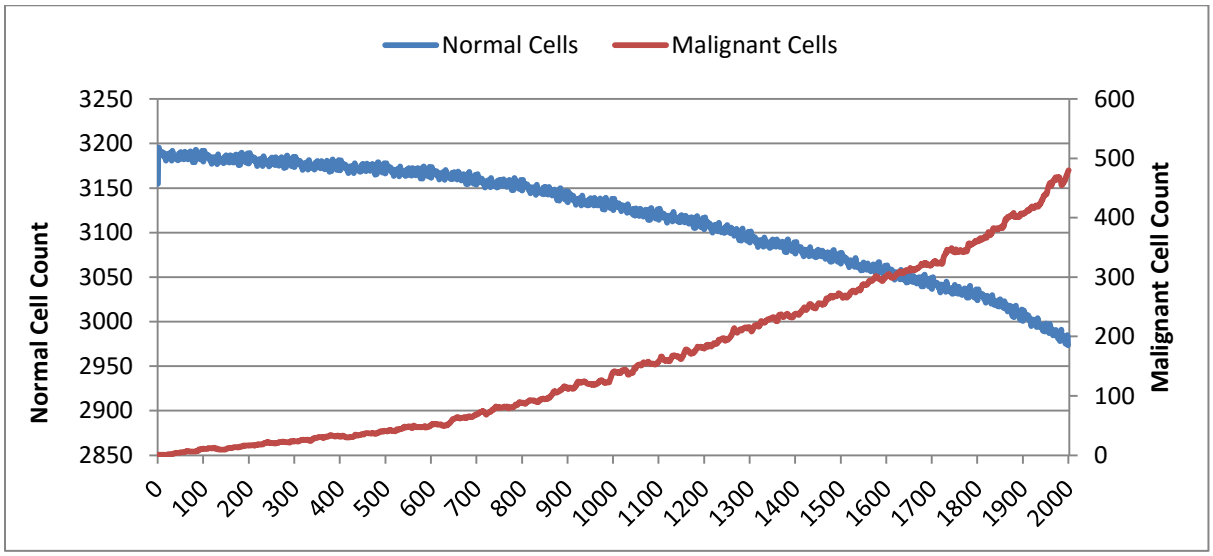

Figure 9 - Change in Normal and Malignant cell counts

In terms of changes in the grid element counts we can plot the change over time of grid elements which only contain Normal cells and those that contain non-Normal cells, as shown in Figure 10. Note that the non-Normal grid elements include those with mixed cell populations, only Malignant cells or those which are classed as Necrotic.

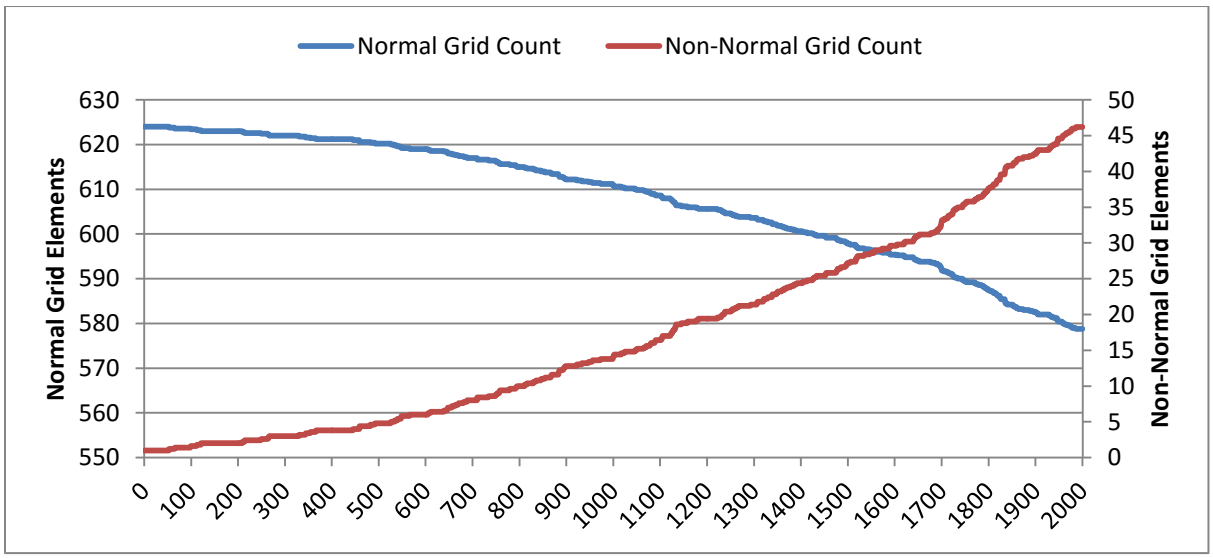

Figure 10 - Change in Normal and Non-Normal Grid Element Counts

Changes in grid elements and cell populations are not the only metrics of interest. Also of interest is the process of evolutionary change in the Malignant cell populations. Our starting point has been that Malignant cells have the same structure as Normal cells, but they are endowed with proliferative and mutational properties. In terms of the initial population there is only a single genotype in the entire population, it is of interest to track how this changes over

PeerJ PrePrints | https://doi.org/10.7287/peerj.preprints.1558v1 | CC-BY 4.0 Open Access | rec: 3 Dec 2015, publ: 3 Dec 2015

time. As shown in Figure 11 the rate of change of the gene pool rises over time and increases in line with the increase in Malignant cell population and the process of invasion. Also shown in Figure 11 is the rise in the number of clonal sub-populations, reflecting the growth of different active Malignant cells populations in the tumour mass.

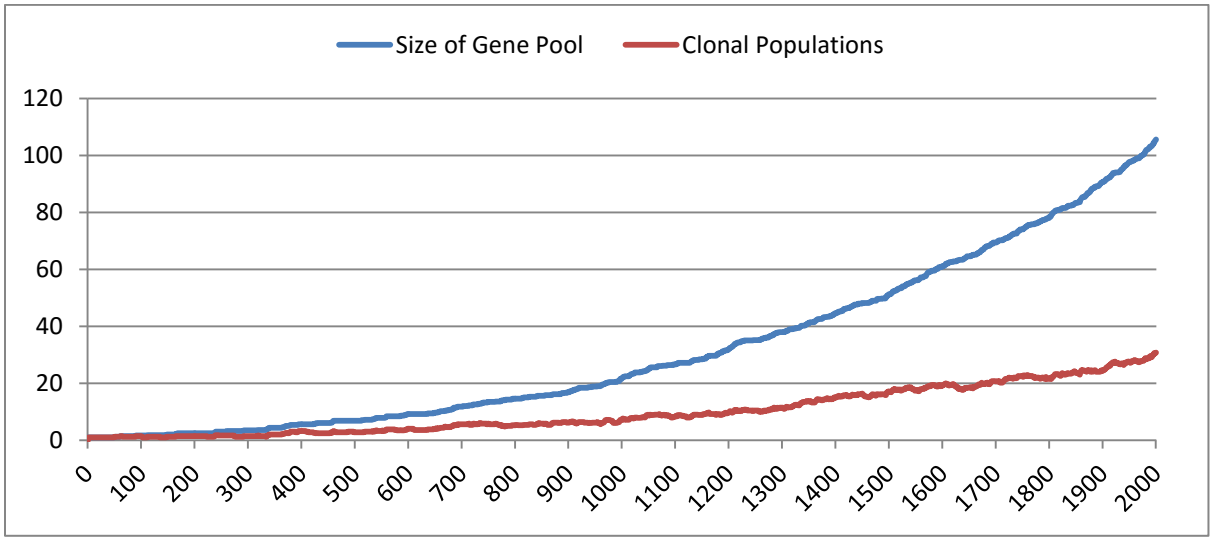

Figure 11 - Change in Gene Pool and Clonal Populations Over Time

To gain further insight into the process of evolutionary change we can also chart the change in fitness levels in both Normal and Malignant cells. Initially the 'seeded' Malignant cell has the same fitness as the Normal cells in the grid element into which it is inserted, however as the number of cells increases, the number of mutations rises, Malignant cells proliferate into neighbouring grid elements and competition for Nutrient and Gene Factors takes place. Fitness, as defined is in the range [0,1], and the change over time is shown in Figure 12.

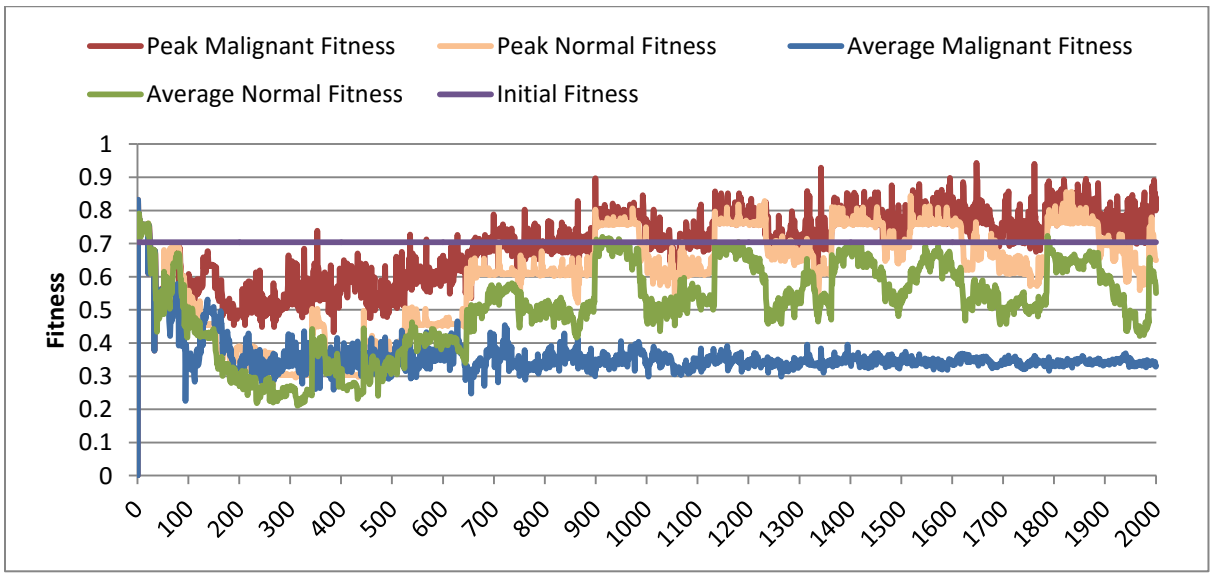

Figure 12 - Change In Fitness Over Time

PeerJ PrePrints | https://doi.org/10.7287/peerj.preprints.1558v1 | CC-BY 4.0 Open Access | rec: 3 Dec 2015, publ: 3 Dec 2015

The noisy signals indicate a good deal of change and adaptation taking place over time. Significantly it is clear that the initial high fitness value is degraded once the cell populations start to increase and competition takes place. It is also clear that the Normal cell population retains an average fitness that is higher than the average fitness of the Malignant cell population. One plausible explanation is that many of the mutations that take place are deleterious and do not lead to improved survival for those cells. However, if we look at the maximum values for the Malignant cells we can see that there are indeed some cells which do achieve a higher fitness than maximum values for the Normal cells.

We can also view the average and maximum number of mutations per Malignant cell over time, again as a measure of the degree of evolutionary change. This is shown in Figure 13. As can be seen for the first 100 generations or so there are no mutations, which accords with Figure 11.

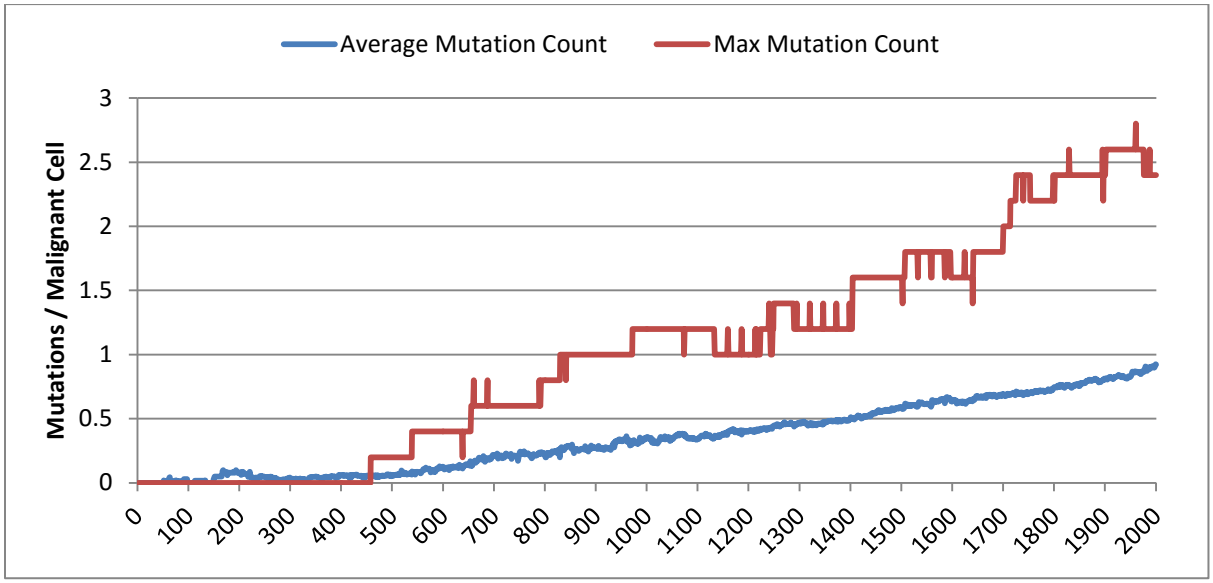

Figure 13 - Mutations per Malignant Cell

We can examine the different cellular components to identify the loci of mutational change over time. The mutation rate and the invasion rate, which are both mutable characteristics, do show some change, as can be seen in Figure 14. Interestingly we see that while initially there is little change, indeed both rates dip below the starting values, both rates show an increasing trend over time. However, the scale of the increase in both these metrics is relatively low and neither rises monotonically.

PeerJ PrePrints | https://doi.org/10.7287/peerj.preprints.1558v1 | CC-BY 4.0 Open Access | rec: 3 Dec 2015, publ: 3 Dec 2015

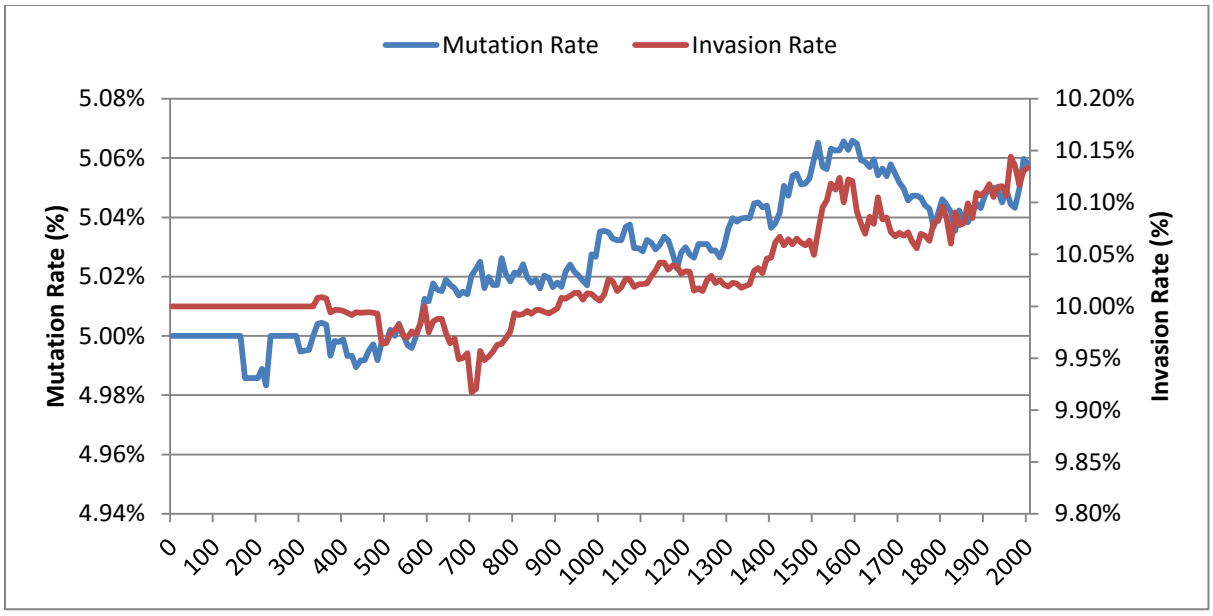

Figure 14 - Change in Mutation and Invasion Rates

The metabolic demands of the Malignant cells are defined by the Nutrient Target and the Nutrient Rate, and these are shown in Figure 15. While the increasing metabolic demand is clear from the rising Nutrient Target value, the Nutrient Rate value shows no longer term increase. Note also that the lower limit of the Nutrient Rate is clear – by definition the Nutrient Rate is a non-zero integer value.

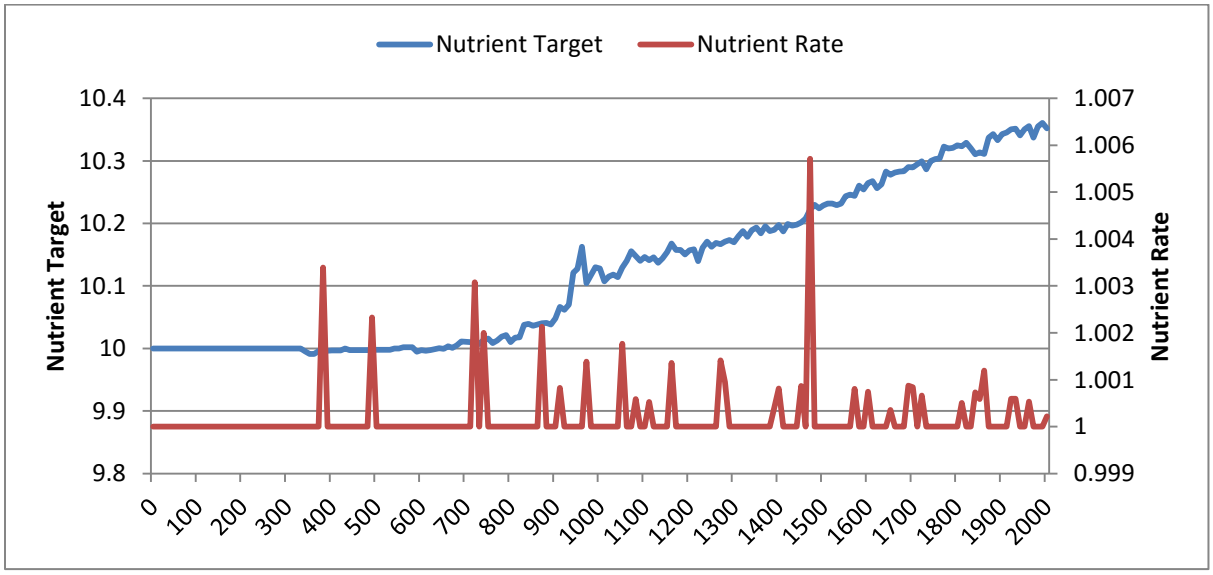

Figure 15 - Change in Malignant Cell Metabolism

PeerJ PrePrints | https://doi.org/10.7287/peerj.preprints.1558v1 | CC-BY 4.0 Open Access | rec: 3 Dec 2015, publ: 3 Dec 2015

There is also evolutionary change in terms of the Genome. To simplify the exposition only one of the three genes is shown in this discussion although the scale and direction of change in the other two genes in our example system are similar. Each of the three genes was defined as having a Target value of 5.0 and a Tolerance value of 1.0. The change in time for the first of these genes is shown in Figure 16. Both the Target and Tolerance values show a fast and sustained decrease in average value.

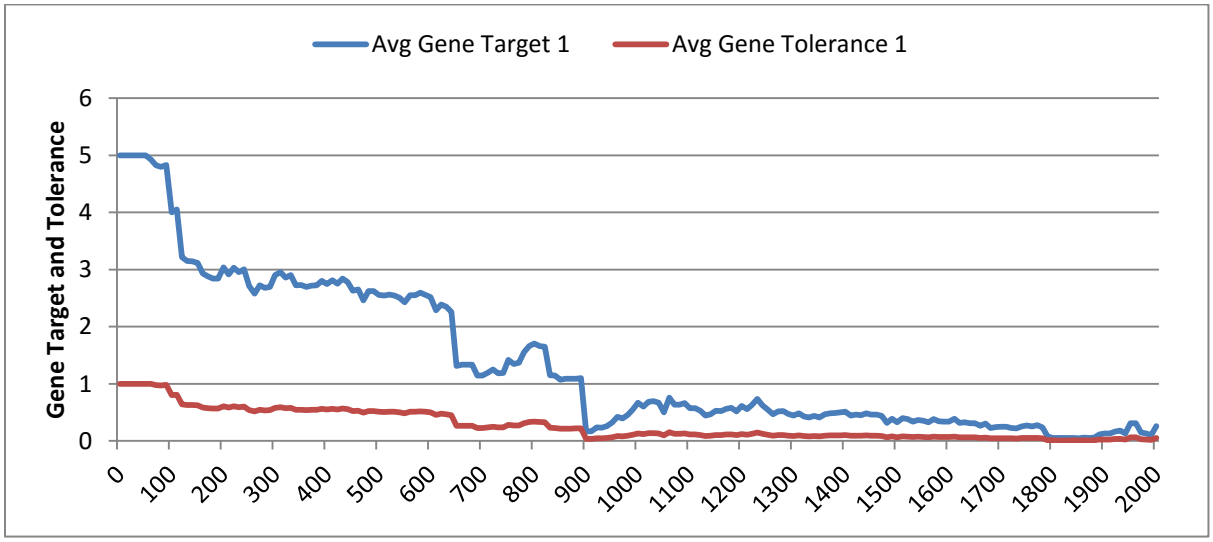

Figure 16 - Change in Gene over time

Gene Expression also shows a marked change over time, which we can see in Figure 17, which also displays the close correlation with the degree of cell turnover in the Malignant population. Given that Gene Expression is a factor in the aging of the cells then this is as we would expect.

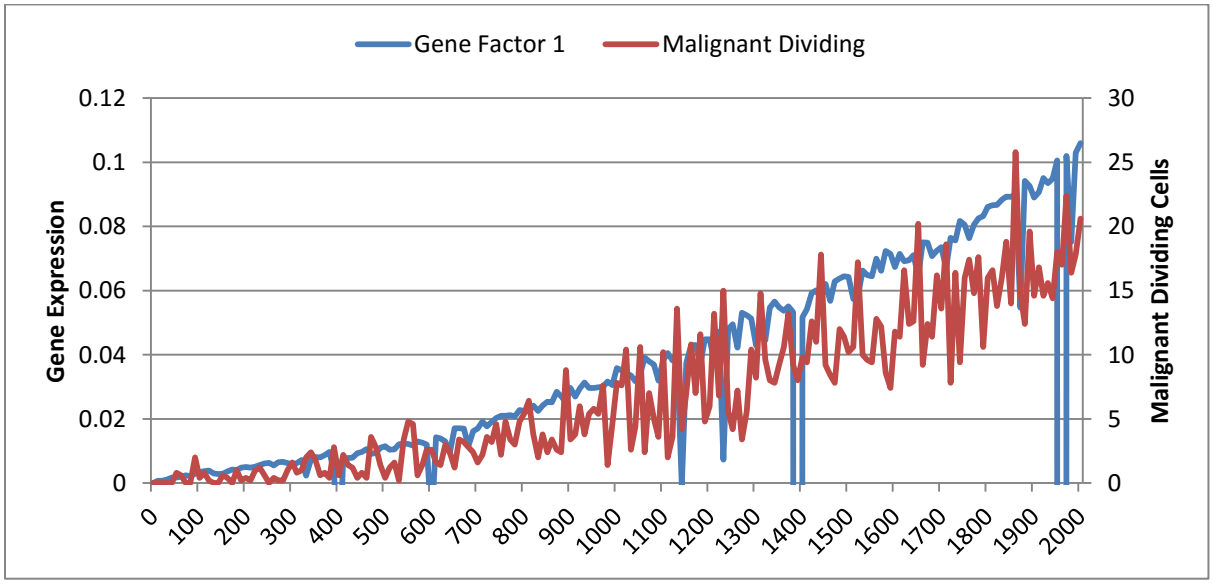

Figure 17 - Gene Expression over Time

PeerJ PrePrints | https://doi.org/10.7287/peerj.preprints.1558v1 | CC-BY 4.0 Open Access | rec: 3 Dec 2015, publ: 3 Dec 2015

Finally, while we have explored the rates of change at the cellular and grid element levels, we have not explored the spatial distribution of the spread of Malignant cells. A representative example of the 'no treatment' scenario is shown in Figure 18, an extended run of 6000 generations and a grid size of 45 x 45 has been used to illustrate more fully the development of the tumour mass over time.

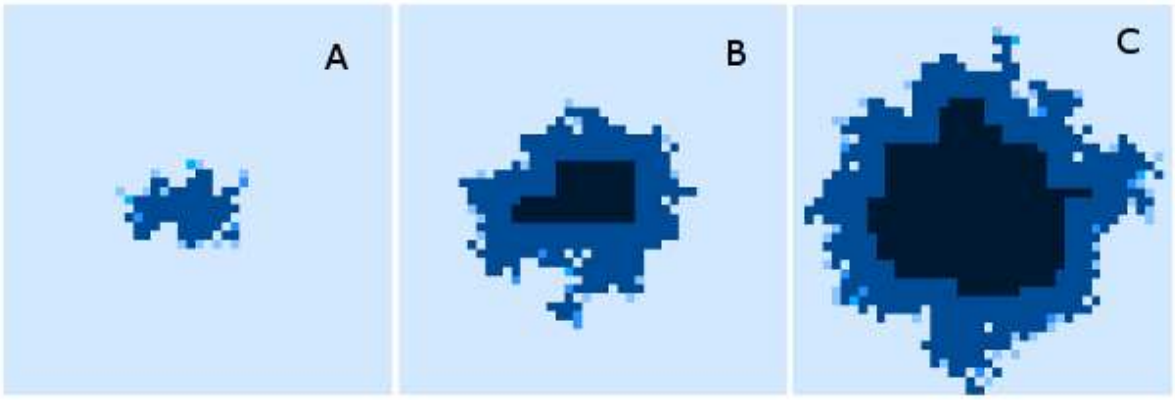

Evolving tumour mass at A: 2000 generations, B: 4000 generations, C: 6000 generations. Note that black areas are necrotic grid elements.

Figure 18 - Spatial distribution of tumour growth

This first set of data used a Mutation Rate of 5% and an Invasion Rate of 10%, we can vary these in turn to understand the impact they have on tumour growth. First we will vary the Mutation Rate from 2.5% to 30% in increments of 2.5%, all other settings are as before. Figures shown are the average of 10 runs of the system. Note that while figures are shown for the final time point of 2000 generations, these values are representative of the trends apparent at earlier time points.

Whether we look at tumour progression in terms of grid elements, as in Figure 19, or in terms of Malignant Cell counts, as in Figure 20, it is clear that there is no direct relationship between mutation rate and tumour progression.

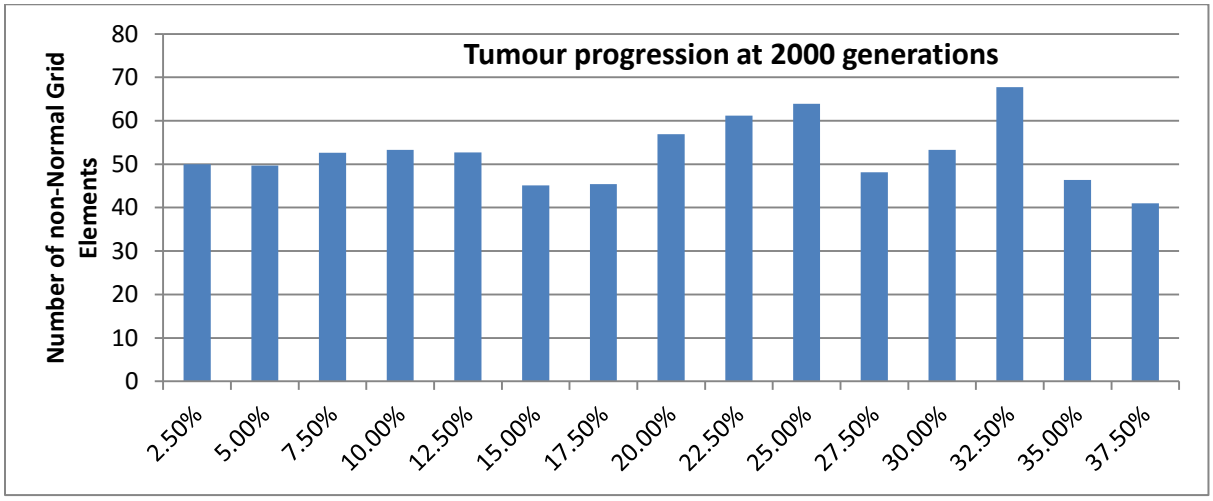

Figure 19 - Number of non-Normal Grid Elements vs Mutation Rate

PeerJ PrePrints | https://doi.org/10.7287/peerj.preprints.1558v1 | CC-BY 4.0 Open Access | rec: 3 Dec 2015, publ: 3 Dec 2015

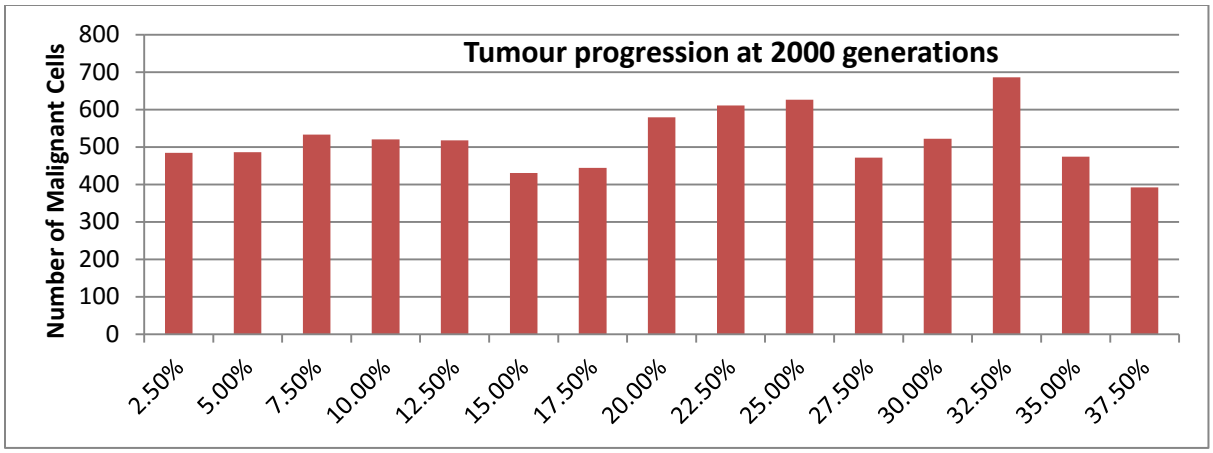

Figure 20 - Number of Malignant Cells vs Mutation Rate

Where we would expect to see a relationship is in the number of mutation events that occur, and here we can view a clear correlation between the mutation rate and the size of the Gene Pool, as shown in Figure 21, though even here the relationship is not completely linear as a mutation rate of 32.5% generated a larger gene pool than a mutation rate of 37.5%.

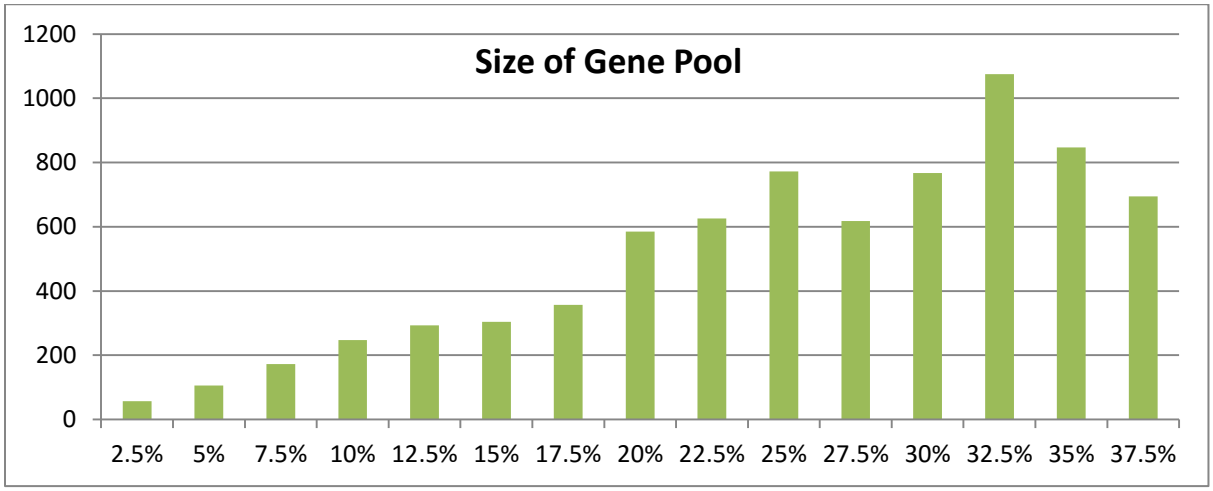

Figure 21 - Size of Gene Pool vs Mutation Rate

Similarly, if we look at the number of clonal sub-populations, as shown in Figure 22, we can see a correlation with the mutation rate, but again this is not linear.

PeerJ PrePrints | https://doi.org/10.7287/peerj.preprints.1558v1 | CC-BY 4.0 Open Access | rec: 3 Dec 2015, publ: 3 Dec 2015

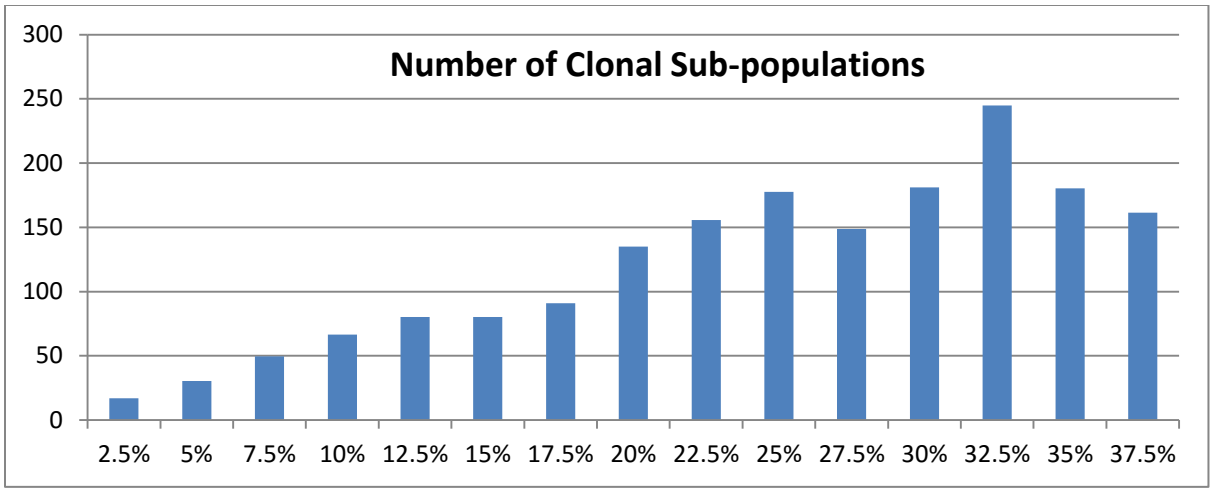

Figure 22 - Number of Clonal Sub-populations vs Mutation Rate

Another interesting metric is the degree of dominance of any one of the clonal sub-populations, which is shown in Figure 23. This shows the percentage of the total number of Malignant cells which belong to the largest clonal sub-population. As is clear from Figure 23, a lower mutation rate yields a greater degree of dominance by a single clonal sub-population.

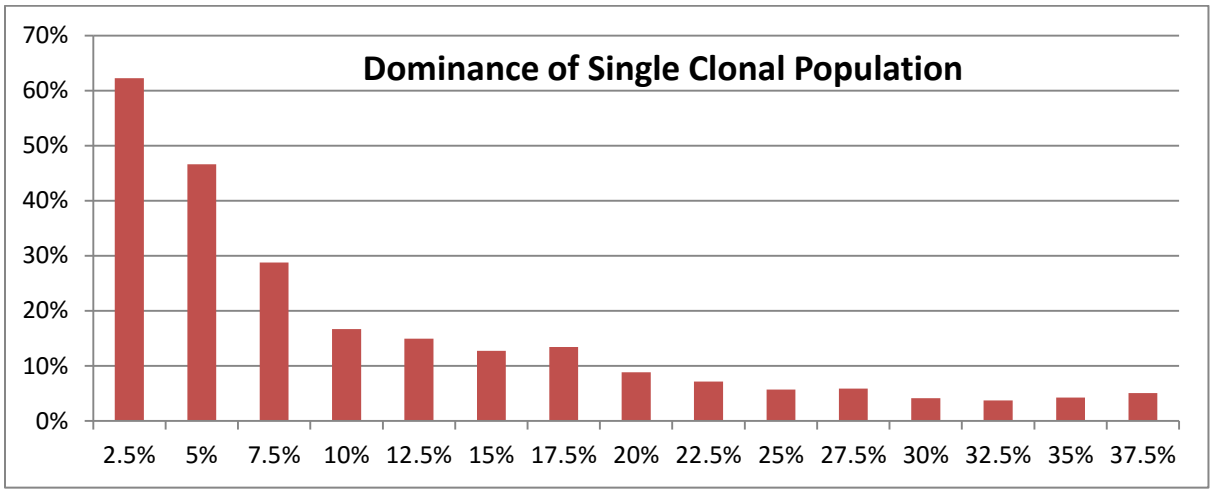

Figure 23 - Dominance of Single Clonal Population vs Mutation Rate

We can also vary the Invasion Rate to see what impact this has on the degree of tumour growth and the size of the gene pool. In this experiment the Invasion Rate is varied from 2% to 20% in 2% increments, the Mutation Rate of 5% is used; all other settings are as before. Figures shown are the average of 10 runs of the system.

Clearly, as shown in Figure 24 and Figure 25, in this case there is a direct relationship between the Invasion Rate, (which is the probability of a migration event in the case when a Malignant cell divides and the grid element already contains a full complement of cells), and the rate of tumour growth. More migration events clearly correlate closely with increased tumour spread.

PeerJ PrePrints | https://doi.org/10.7287/peerj.preprints.1558v1 | CC-BY 4.0 Open Access | rec: 3 Dec 2015, publ: 3 Dec 2015

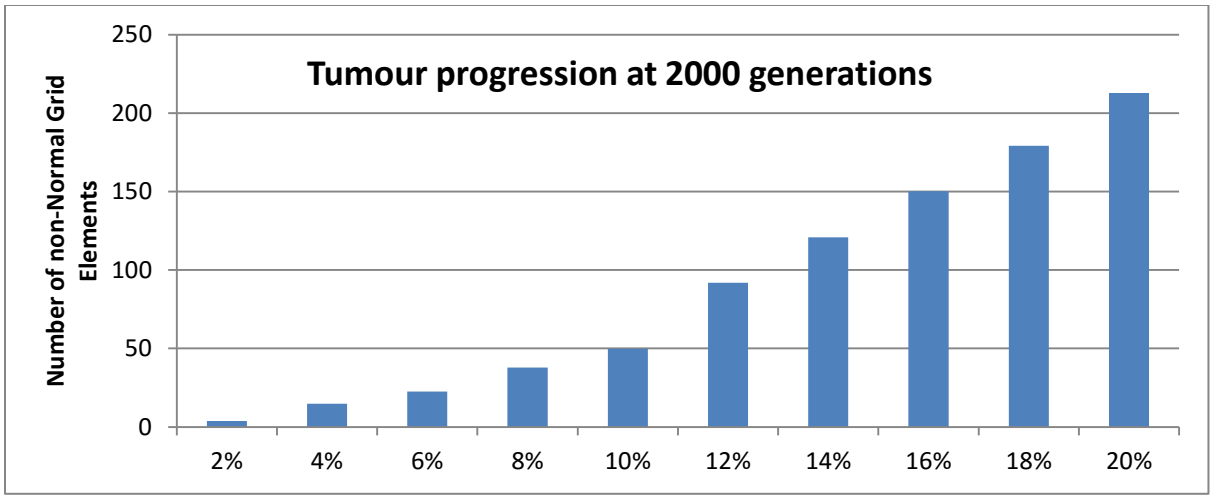

448

449 **Figure 24 - Number of non-Normal Grid Elements vs Invasion Rate**

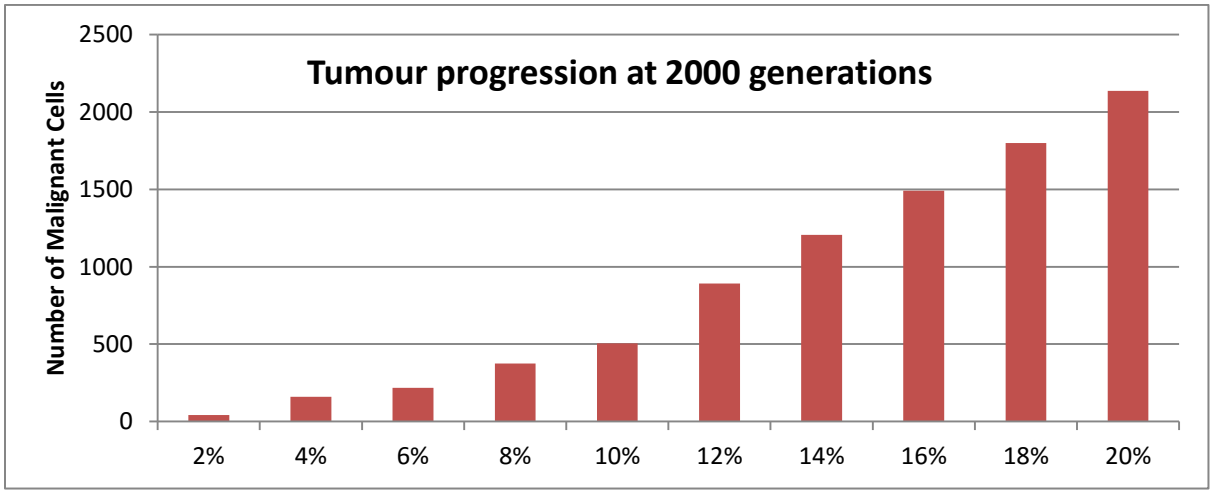

450

451 **Figure 25 - Number of Malignant Cells vs Invasion Rate**

452 This increased rate of tumour growth, both in terms of grid elements and number of Malignant
453 cells, also leads to an increase in the size of the Gene Pool, shown in Figure 26. However, when
454 compared to the scale of the increase of the Gene Pool with a rising Mutation Rate, as shown in
455 Figure 21, it is clearly lower and indicates a less heterogeneous Malignant cell population.

PeerJ PrePrints | https://doi.org/10.7287/peerj.preprints.1558v1 | CC-BY 4.0 Open Access | rec: 3 Dec 2015, publ: 3 Dec 2015

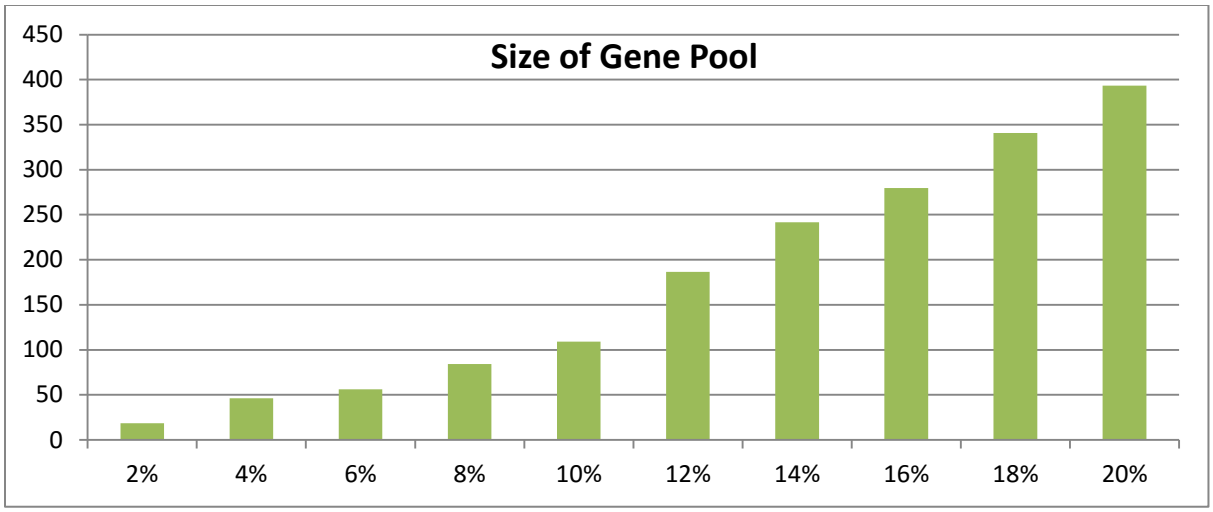

Figure 26 - Size of Gene Pool vs Invasion Rate

In terms of the dominance of a single clonal population, shown in Figure 27, a lower Invasion rate is associated with an increased dominance by a single clonal sub-population, but even at a high Invasion Rate of 20% the degree of dominance is much higher than associated with a high Mutation Rate.

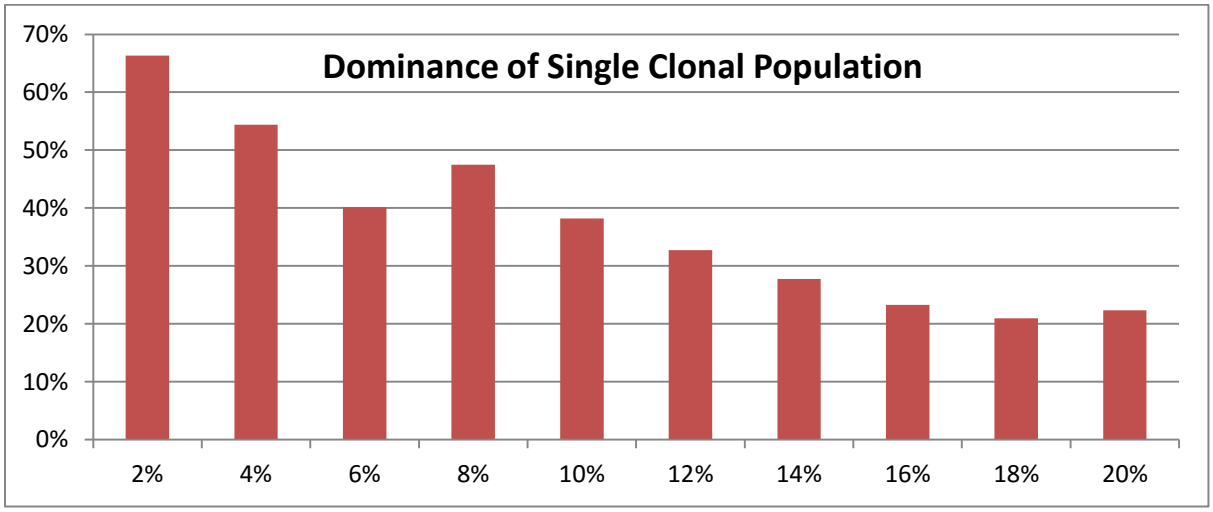

Figure 27 - Dominance of Single Clonal Population vs Invasion Rate

Tumour Growth – With Treatment

The previous experiment has detailed the salient features of the NEATG tumour growth process, both in terms of changes in cell populations, grid elements and also in the underlying genetic/evolutionary processes at work. As has been shown, in the absence of any interventions the number of Malignant cells rises and a process of invasion occurs such that Malignant cells are able to move into adjacent grid elements. In the next series of experiments we will investigate the impact on these growth patterns of a number of interventions.

PeerJ PrePrints | https://doi.org/10.7287/peerj.preprints.1558v1 | CC-BY 4.0 Open Access | rec: 3 Dec 2015, publ: 3 Dec 2015

The treatment strategy object is a mechanism by which NEATG can be used to model different intervention strategies and one such strategy, to be explored in this experiment, is loosely based on the example of high-dose cytotoxic chemotherapy. Just as with cytotoxic chemotherapy this is not a targeted therapy – it is applied to both Normal and Malignant cells. Where real chemotherapy causes apoptotic cell death in rapidly dividing cells, the treatment strategy in this model flags cells which are dividing, or which are arbitrarily close to dividing, with the cell state of TO_BE_CLEARED. The arbitrary cut-off is based on the value of a cell's clock and this value is a configurable parameter in the system. By adjusting the cut-off value we can approximate control the 'toxicity' of the treatment, the higher the cut-off value the more toxic the treatment as more cells will be flagged for disposal. The system also allows a degree of specificity in that we can make Malignant cells more susceptible to the treatment than Normal cells.

In the first experiment the same parameters will be used as in the No Treatment scenario. The treatment will commence at generation 1500 (of 2000), and will be applied for 25 generations. In this experiment three different toxicity values are assessed, with both Malignant and Normal having the same cut-off values. The values used are 0, 10 and 20, which means that any cell with a clock value lower than the cut-off is 'treated' in the respective scenarios. Note that the zero cut-off value does not trigger cell division as is the default case without treatment but triggers apoptosis and cell clearance. It does though represent the least toxic scenario and is therefore close to the 'no treatment' scenario. The results shown are the averages for 10 runs of the system.

As can be seen from Figure 28, the effect of treatment on the total cell count is dramatic. In the case of the more toxic treatments, there is a sharp decline in total cell numbers followed by a recovery in cell numbers, and in the case of the highest cut-off value of 20 cell growth accelerates above the pre-treatment trend.

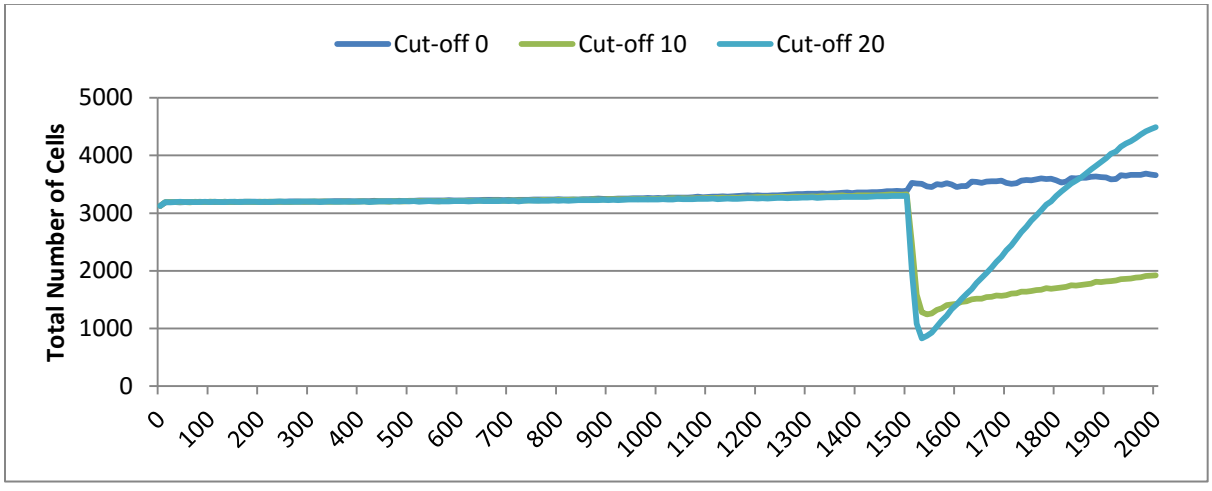

Figure 28 - Total Cell Counts vs Treatment Toxicity

We can also see how this change in growth trajectory is reflected in the Grid Element view of tumour growth, as shown in Figure 29 and Figure 30, which show the Normal and Tumour Grid Elements respectively. In Figure 29 we see that the initiation of treatment leads to a sharp reduction in the number of Normal Grid Elements as the chemotherapy adversely affects Normal

PeerJ PrePrints | https://doi.org/10.7287/peerj.preprints.1558v1 | CC-BY 4.0 Open Access | rec: 3 Dec 2015, publ: 3 Dec 2015

cells, followed by a small period of recovery and then a continued decline in numbers. The corresponding view of Tumour Grid Elements, in Figure 30, shows that the slow rise in number is briefly interrupted when treatment begins but then accelerates sharply after the completion of treatment. Furthermore in both figures we see that the more aggressive treatment in terms of toxicity is related to an increased growth tumour growth rate with the cessation of treatment.

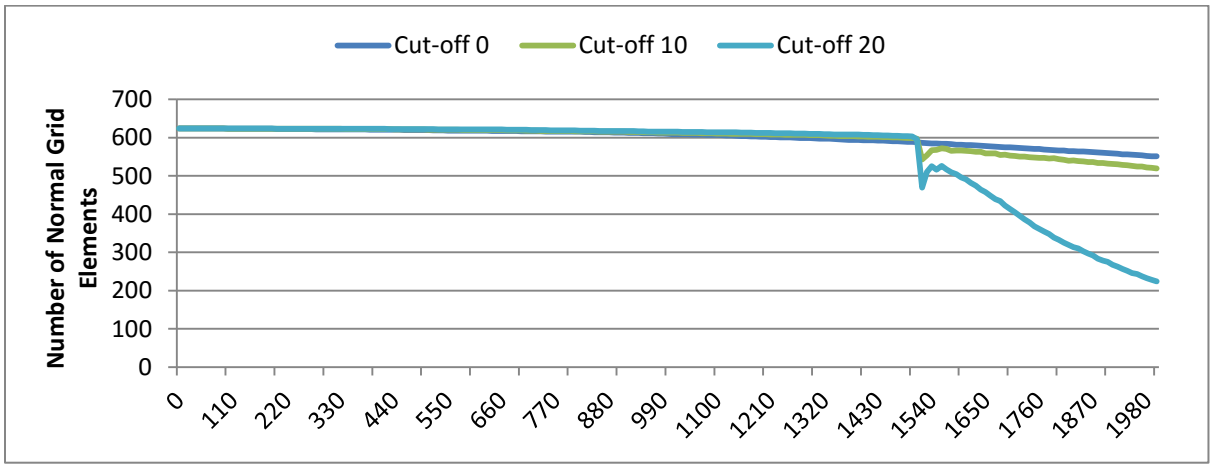

Figure 29 - Normal Grid Elements vs Treatment Toxicity

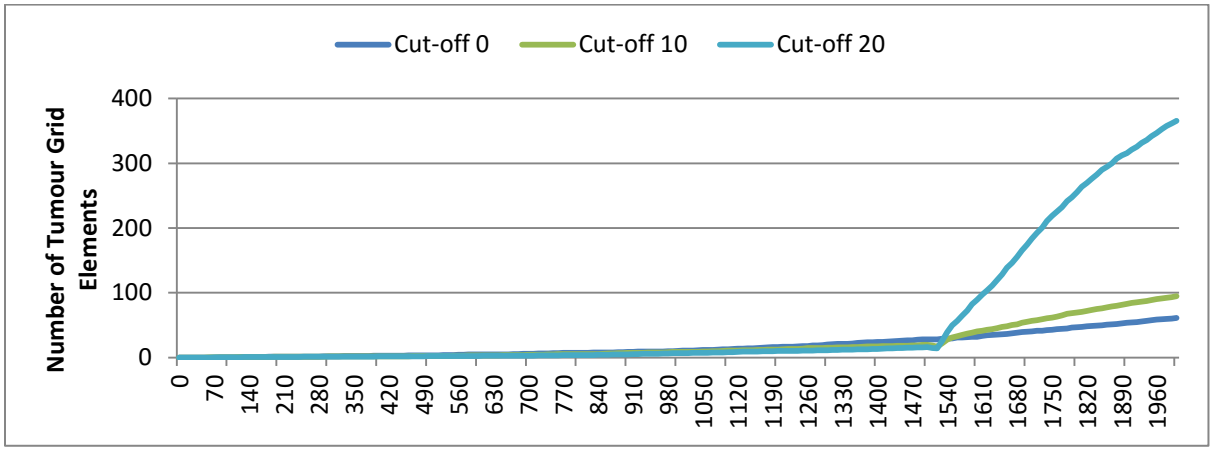

Figure 30 - Tumour Grid Elements vs Treatment Toxicity

To gain more insight into this behaviour we can look at the change in the Normal Cell population, as shown in Figure 31. Here we can see that the treatment induces a sharp reduction in cell numbers, and that this decline continues even after the cessation of treatment, though not at the same rate.

PeerJ PrePrints | https://doi.org/10.7287/peerj.preprints.1558v1 | CC-BY 4.0 Open Access | rec: 3 Dec 2015, publ: 3 Dec 2015

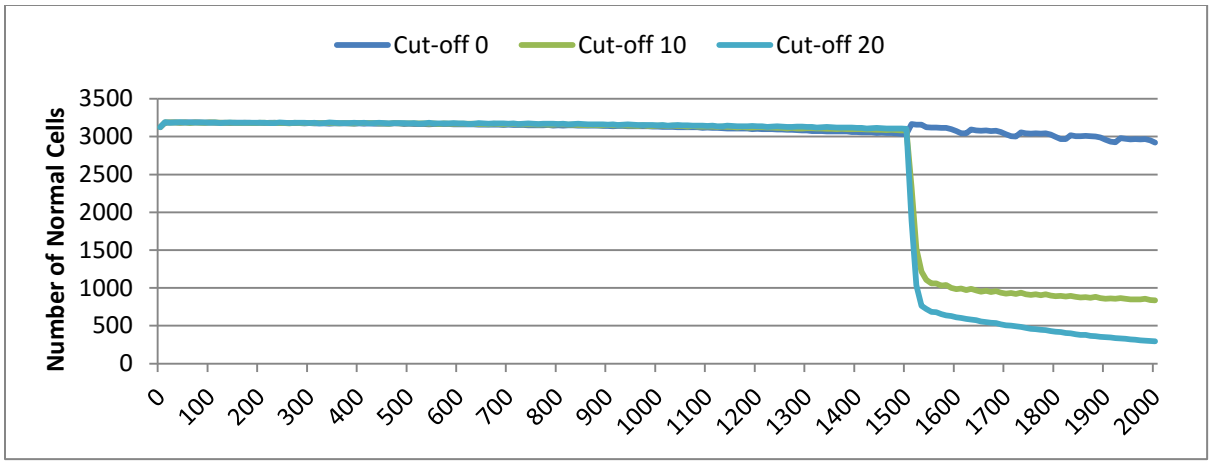

Figure 31 - Normal Cell Population vs Treatment Toxicity

In the case of the Malignant Cells, shown in Figure 32, we also see a decline in cell numbers during the treatment, followed by rapid recovery. We can assume that in this case the decline in Normal cell numbers has provided the conditions in which Malignant cells can expand rapidly in number.

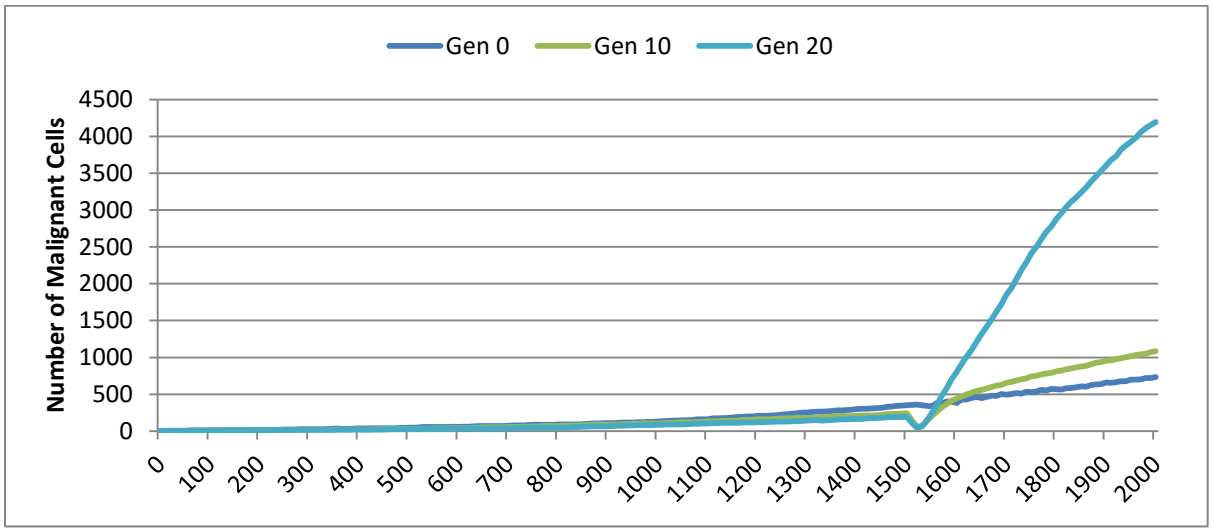

Figure 32 - Malignant Cell Population vs Treatment Toxicity

Supporting evidence is provided by the Gene Pool trends, shown in Figure 33. Here we can see that following treatment there is an increase in the size of the Gene Pool, indicating a post-treatment burst of clonal evolution.

PeerJ PrePrints | https://doi.org/10.7287/peerj.preprints.1558v1 | CC-BY 4.0 Open Access | rec: 3 Dec 2015, publ: 3 Dec 2015

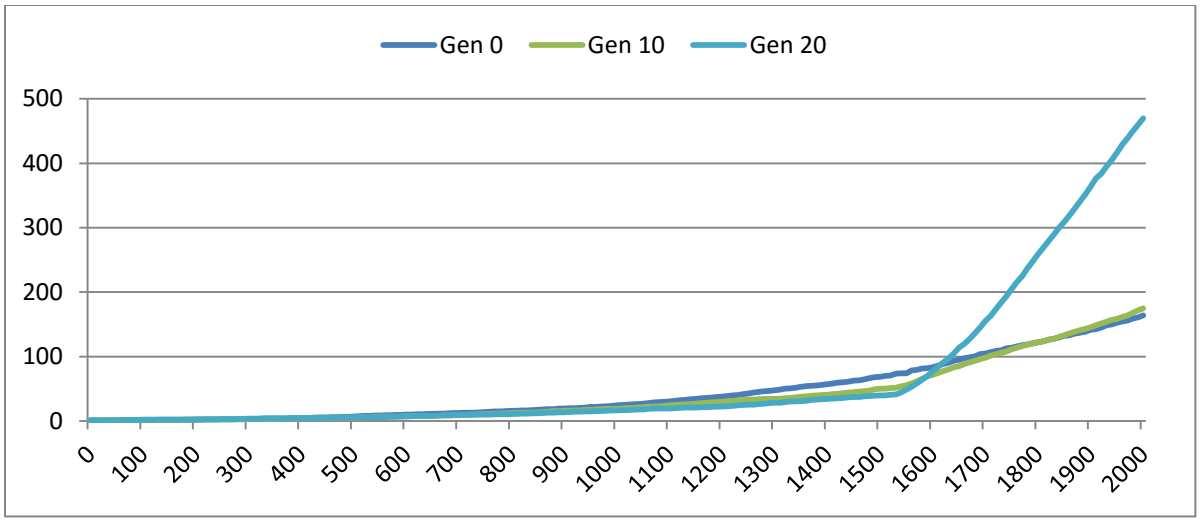

Figure 33 - Size of Gene Pool vs Treatment Toxicity

In terms of the number of active clonal subpopulations, as shown in Figure 34, the same trend emerges. The number of active clonal subpopulations shows a slow increase until generation 1500, at which point treatment commences. Some of these populations are killed by the treatment and we see a dip in numbers, but following the cessation of treatment there is an evolutionary explosion and a rapid rise in the number of clonal sub-populations.

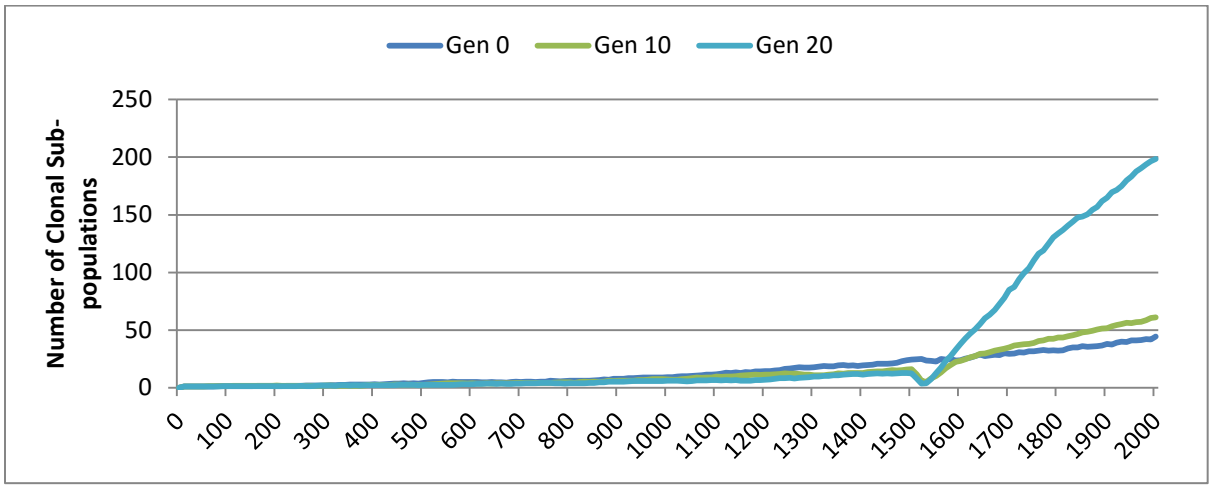

Figure 34 - Number of clonal sub-populations vs Treatment Toxicity

Another view of this evolutionary burst is provided by Figure 35. Here we can see that the process of tumour growth leads to an increase in genetic heterogeneity, as shown by the proportion of the Malignant cell population belonging to the largest sub-population. The increasing heterogeneity is interrupted when the treatment begins and there is a spike which shows that the largest sub-population increases as a proportion of the total, from which we can infer that a number of clonal sub-populations have been exterminated completely, in line with Figure 34.

PeerJ PrePrints | https://doi.org/10.7287/peerj.preprints.1558v1 | CC-BY 4.0 Open Access | rec: 3 Dec 2015, publ: 3 Dec 2015

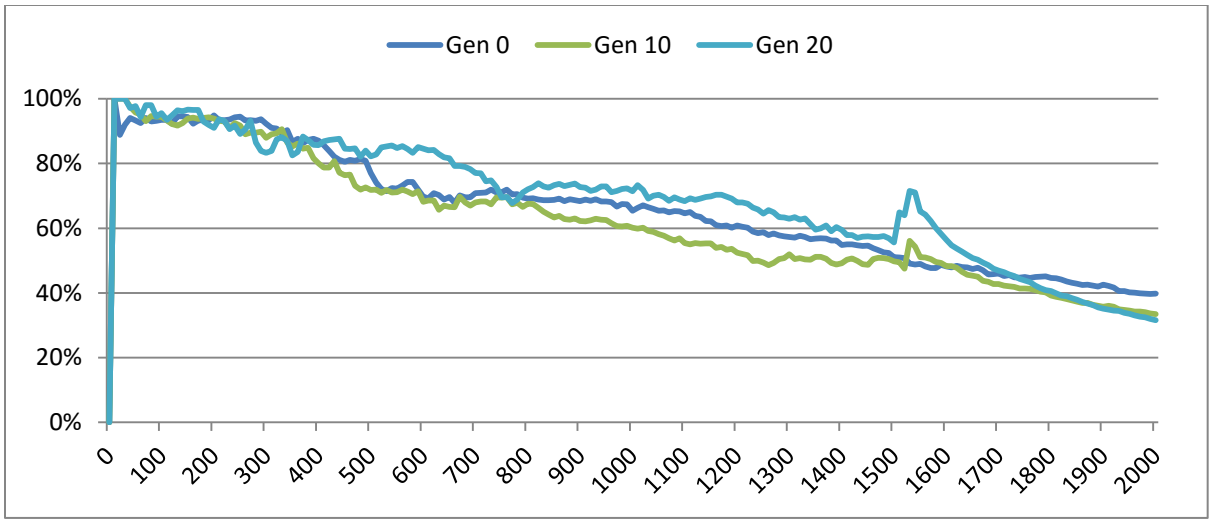

Figure 35 - Sub-clonal Population Dominance vs Treatment Toxicity

In practice maximum tolerated dose (MTD) chemotherapy does not cause equal levels of damage to all cell populations. Because it impacts rapidly proliferating cells the 'collateral damage' to non-tumour cells is restricted to certain populations of non-cancer cells in the immune system, gut and other tissues associated with the side effects of treatment. We can model this differential impact in the NEATG system by setting a lower cut-off value for Normal cells compared to Malignant cells, thus causing fewer Normal cells to be affected by the treatment compared to the Malignant cell populations. In the following experiment the cut-off for the Normal cells is set to 10, and for the Malignant cells it is set to 15, 20 and 25 in three different scenarios. All other parameters are the same as in the previous experiment and the results shown are the averages for 10 runs of the system.

In terms of the total cell counts, shown in Figure 36, there is a similar pattern to the previous experiment, although the rate of recovery is much lower than in Figure 28. The lower sensitivity of the Normal cells means that even when the cut-off for the Malignant cells matches the previous values, the recovery of cell populations is lower.

PeerJ PrePrints | https://doi.org/10.7287/peerj.preprints.1558v1 | CC-BY 4.0 Open Access | rec: 3 Dec 2015, publ: 3 Dec 2015

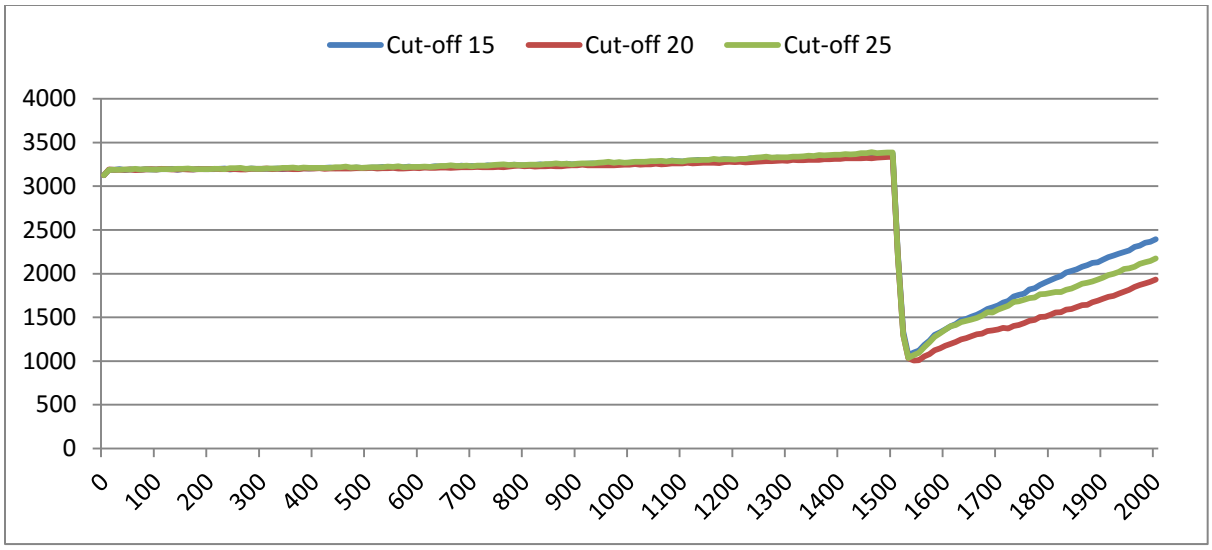

Figure 36 - Total Cell Counts vs Differential Treatment Toxicity

We can also see the impact of treatment on the tumour spread expressed in terms of Grid Elements, as shown in Figure 37.

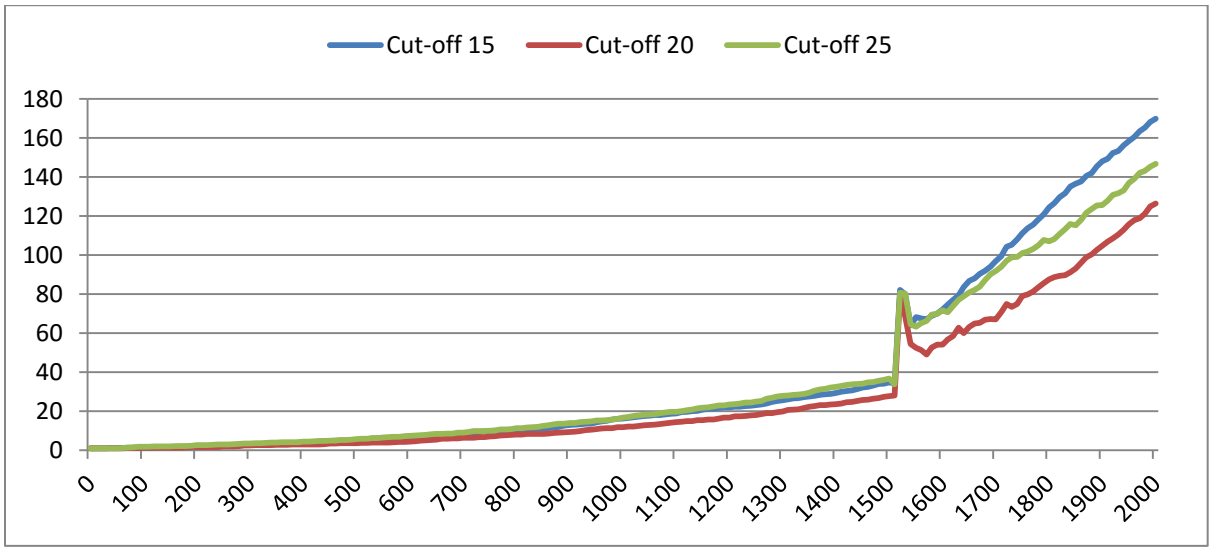

Figure 37 - Tumour Growth vs Differential Treatment Toxicity

The lower sensitivity of the Normal cells does not mean that they are immune from effects of treatment. Figure 38 shows a marked decline in Normal cell numbers on the commencement of treatment, followed by a continued decline after treatment ends. Note there is no difference in the three scenarios shown, indicating that the Normal cells are not affected directly by the different sensitivities of the Malignant cells. We can also see that the values shown here are a close match to those shown for the Cut-off 10 scenario illustrated in Figure 31.

PeerJ PrePrints | https://doi.org/10.7287/peerj.preprints.1558v1 | CC-BY 4.0 Open Access | rec: 3 Dec 2015, publ: 3 Dec 2015

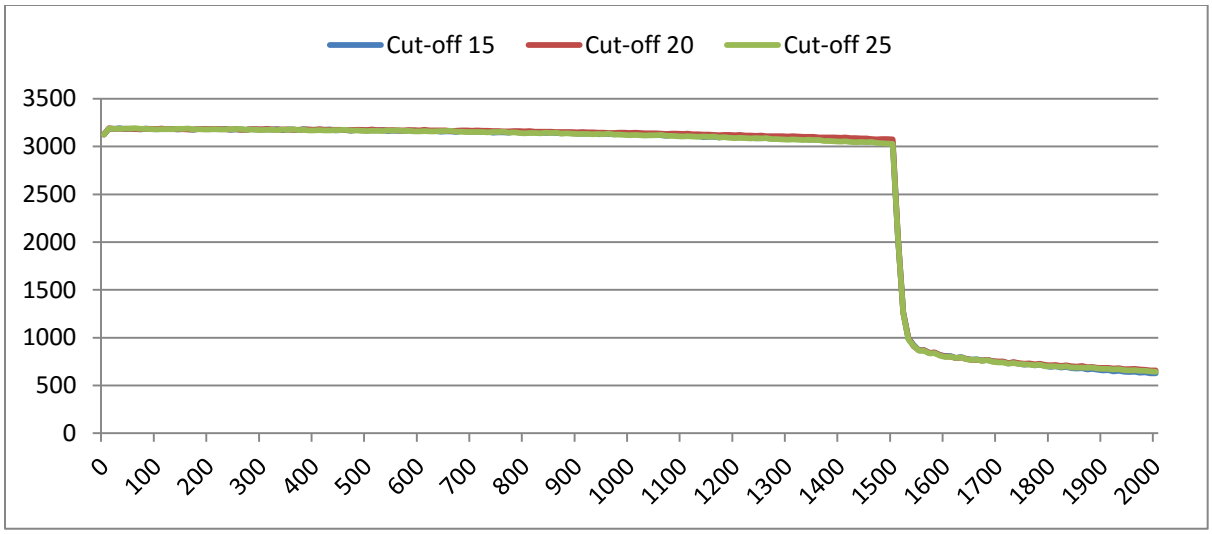

Figure 38 - Normal Cell Counts vs Differential Treatment Toxicity

Finally, the pattern of increased tumour growth and evolutionary change following the cessation of treatment also occurs, as shown in Figure 39.

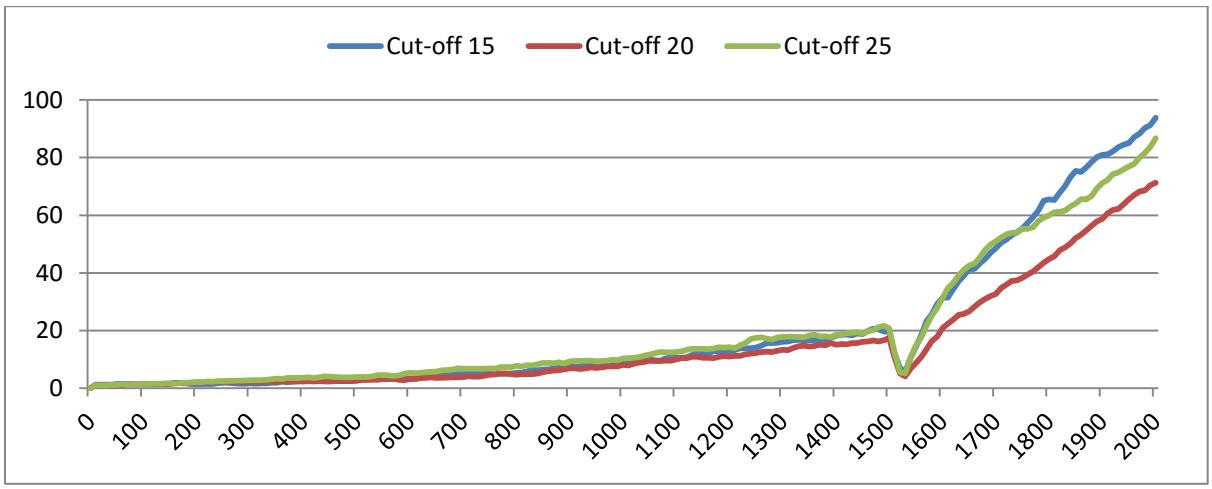

Figure 39 - Clonal Populations vs Differential Treatment Toxicity

Two rather obvious questions arise from this data. The first is what happens if the period of treatment is extended? It is clear that for the duration of treatment the number of Malignant cells, tumour grid elements and clonal populations decrease. Is it possible to extend the treatment period so that the entire Malignant cell population is destroyed? Secondly, it is clear that the treatment damages Normal cells and that this coincides with the increased cancer growth following the cessation of the treatment. Therefore we can ask what happens in the case when the differential toxicity is such that there is no damage to the Normal cells – in other words what would happen in the case of a 'magic bullet' which has toxic effects only on Malignant cells? These questions are addressed in turn in the next two of experiments.

In the following experiment a differential toxicity was used, with a Malignant cut-off value of 20 and a Normal value of 10. All other settings are as in the previous experiment, with the

PeerJ PrePrints | https://doi.org/10.7287/peerj.preprints.1558v1 | CC-BY 4.0 Open Access | rec: 3 Dec 2015, publ: 3 Dec 2015

exception of the treatment duration which was varied from 15 – 60 generations, in increments of 5. The results shown are the averages of 10 runs of the system.

In terms of the total cell counts, we can see that there is indeed a relationship between the treatment length and the size of the total cell population, as shown in Figure 40. It is clear that this is a complex and non-linear relationship, but it is apparent that treatment duration above 40 causes high levels of cell damage. This result was robust to repeated runs of the system and there was essentially no difference between results for any treatment length above this level. Furthermore, this upper cut-off figure for treatment length was related to the length of the cell Lifetime (which is 100 in these experiments). In order to simplify the exposition, the rest of the results in this experiment will focus on treatment lengths of 20 – 35.

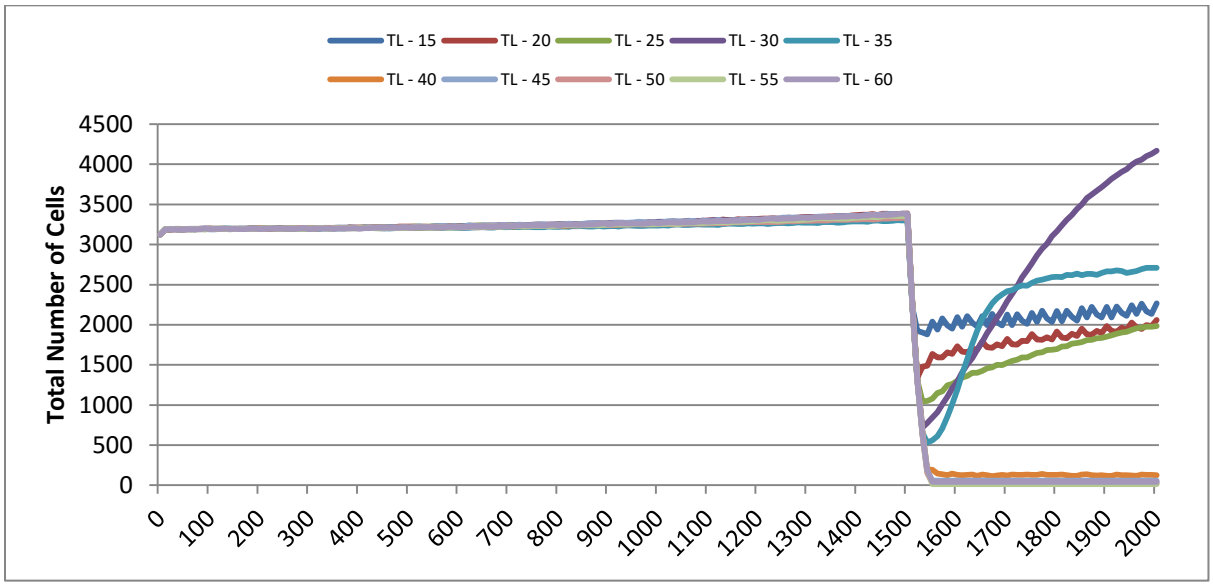

Figure 40 - Total cell count vs treatment length

The effect of treatment length on the Normal and Malignant cell populations is shown in Figure 41 and Figure 42 respectively. In the case of the Normal cell populations it is clear that increasing treatment length is strongly associated with the scale of the decline in cell numbers. However, in the case of the Malignant cells, the treatment length is also associated with the rate of recovery.

PeerJ PrePrints | https://doi.org/10.7287/peerj.preprints.1558v1 | CC-BY 4.0 Open Access | rec: 3 Dec 2015, publ: 3 Dec 2015

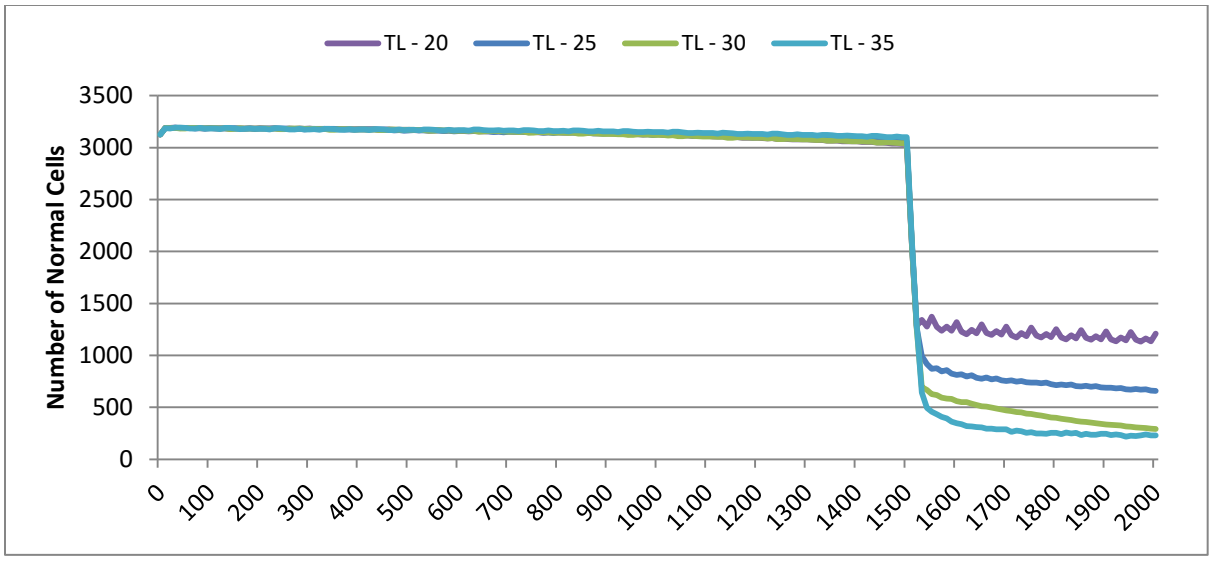

605

606 **Figure 41 - Normal cell count vs treatment length**

607

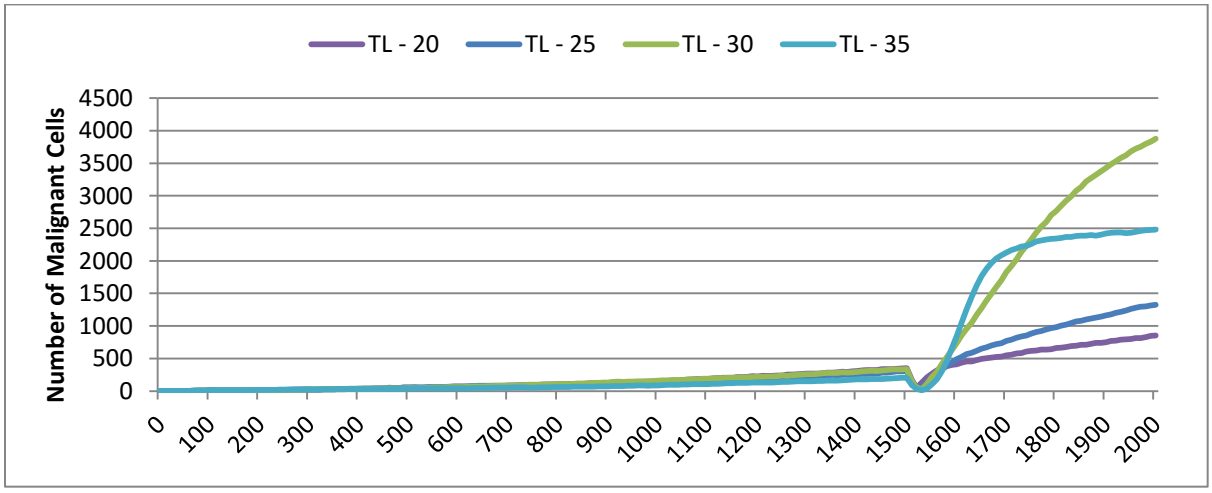

608

609 **Figure 42 - Malignant cell population vs treatment length**

610 As shown in Figure 42 the longer treatment length can sometimes lead to an accelerated increase
611 in Malignant cell numbers, though for treatment lengths beyond 40 (data not shown), there is no
612 recovery in cell numbers, as should be clear from Figure 40 which indicates a collapse in the
613 total cell count. The somewhat surprising result is that in some cases a more aggressive treatment
614 (longer treatment period) can lead to an unexpected acceleration in tumour growth. This is also
615 apparent in Figure 43, which shows the Grid Element view, again with a decline in tumour extent
616 immediately following treatment followed by a recovery that is related to the treatment length.

PeerJ PrePrints | https://doi.org/10.7287/peerj.preprints.1558v1 | CC-BY 4.0 Open Access | rec: 3 Dec 2015, publ: 3 Dec 2015

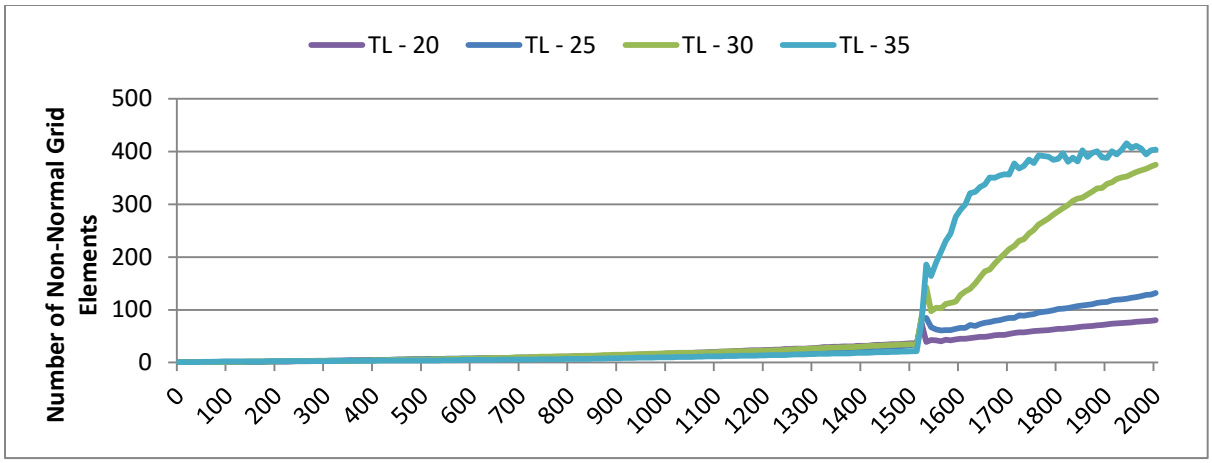

Figure 43 - Non-Normal grid elements vs treatment length

We can also see from Figure 44 that treatment length is also associated with an increase in the size of the Gene Pool. Treatment period therefore acts as a spur to clonal evolution, as also shown in Figure 45.

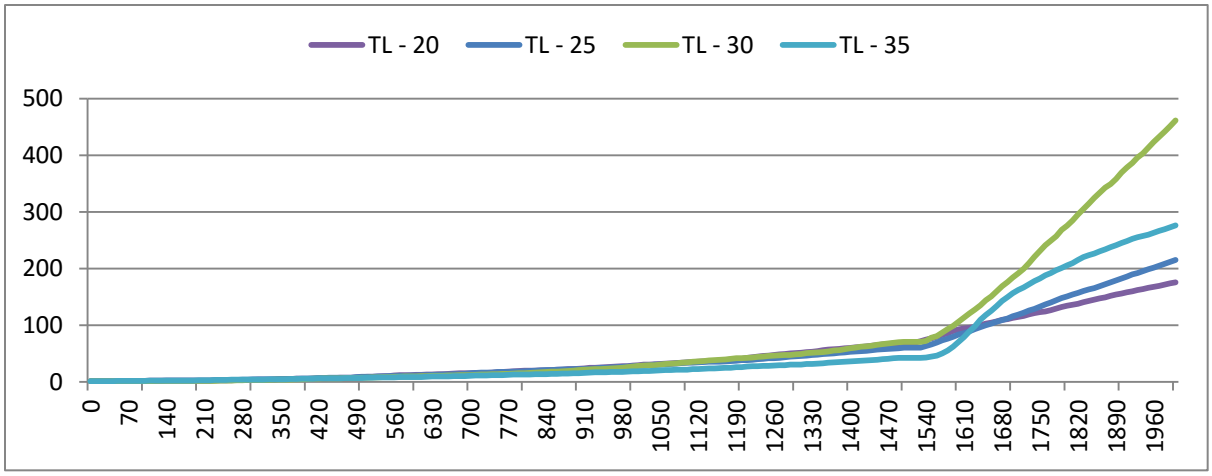

Figure 44 - Gene Pool vs Treatment Length

PeerJ PrePrints | https://doi.org/10.7287/peerj.preprints.1558v1 | CC-BY 4.0 Open Access | rec: 3 Dec 2015, publ: 3 Dec 2015

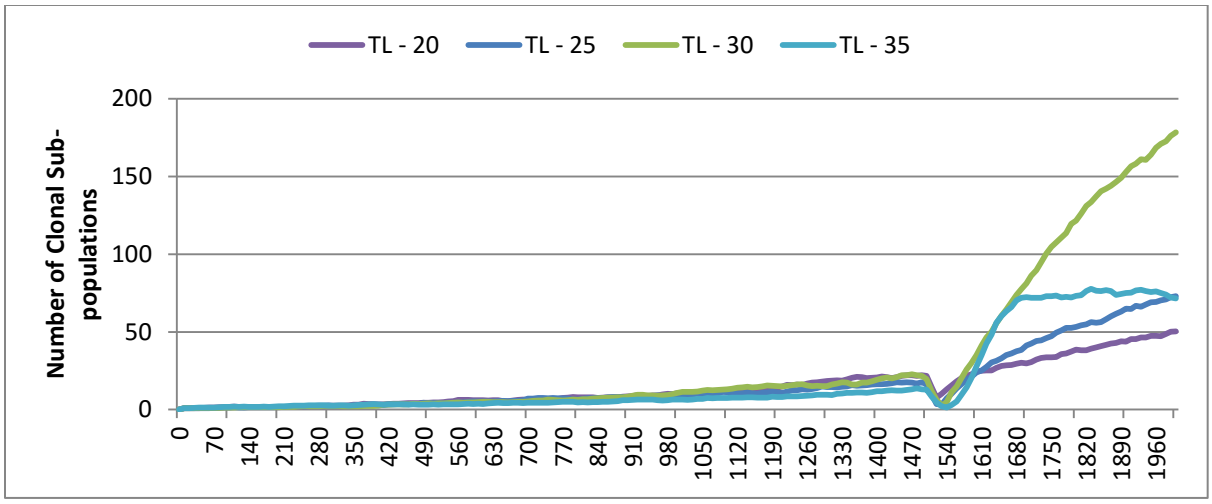

Figure 45 - Clonal populations vs treatment length

A further indication of the effect that treatment length has on clonal evolution is shown in Figure 46, which charts the percentage of the total Malignant population which belong to the most populous clonal sub-population. It is clear that longer treatment length increases dominance as cells from less popular genotypes are removed, whereas for the short treatment of 20 generations there is no such spike in dominance.

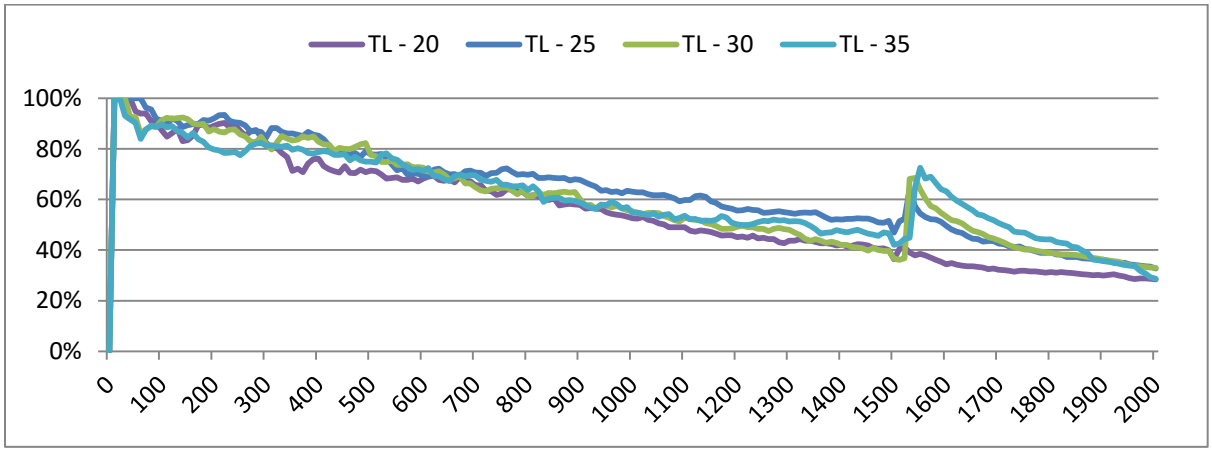

Figure 46 - Sub-clonal dominance vs treatment length

In the final experiment in this section we investigate a scenario where the treatment is applied only to Malignant cells and Normal cells are not affected at all. In this experiment three different toxicity levels are applied to the Malignant cells, representing cut-off values of 15, 20 and 25. All other parameters are as in the previous experiments and the average of 10 runs is shown.

In stark contrast to Figure 28 and Figure 36, treatment does not lead to a sharp decline in total cell numbers, as shown in Figure 47. This is confirmed when we look at the Normal cell numbers, Figure 48. Here we can see a slow decline in numbers prior to the commencement of treatment at generation 1500, followed by a recovery in numbers and then a slow decline again.

PeerJ PrePrints | https://doi.org/10.7287/peerj.preprints.1558v1 | CC-BY 4.0 Open Access | rec: 3 Dec 2015, publ: 3 Dec 2015

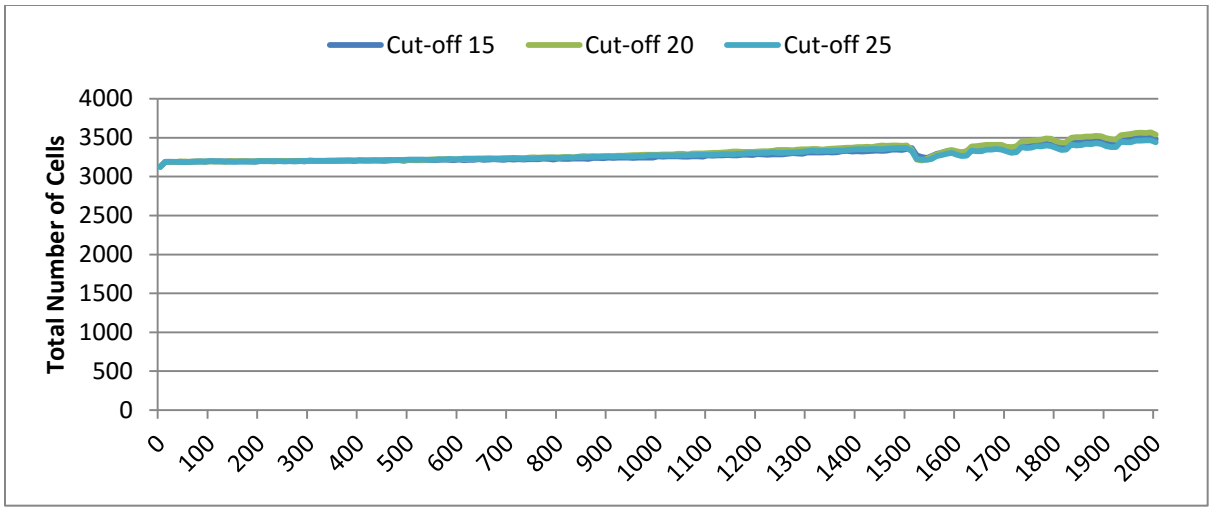

641

642 **Figure 47 - Total cell count vs no collateral damage**

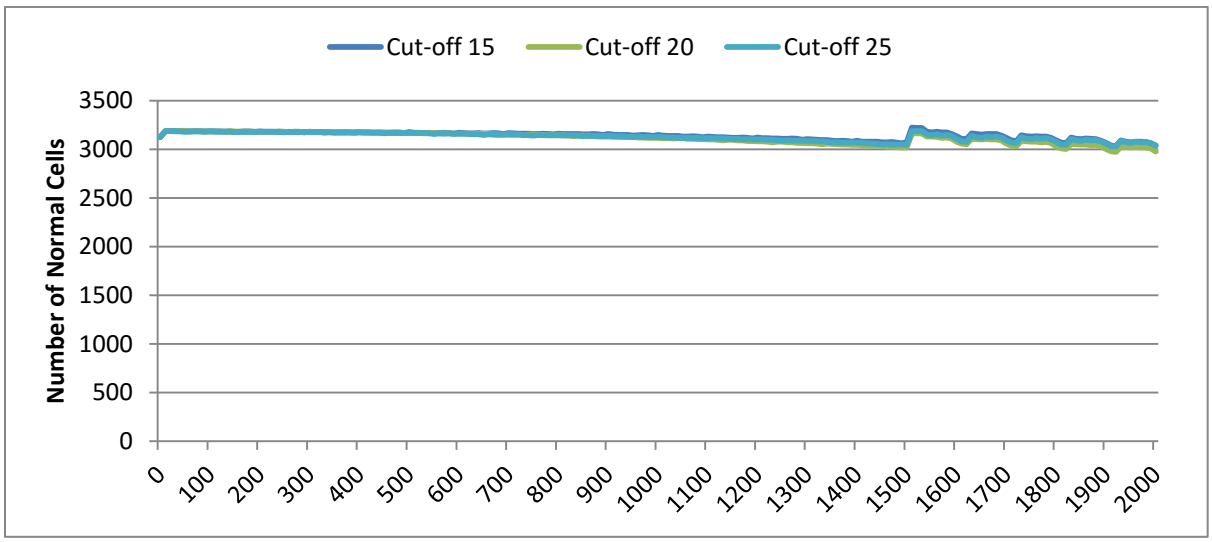

643

644 **Figure 48 - Normal cell numbers vs no collateral damage**

645 In contrast the impact of treatment in clear on the Malignant cell numbers, as shown in Figure
646 49. Here we can see that the increase in cell numbers is reversed sharply by the treatment but is
647 then followed by a recovery in numbers and a resumption of tumour growth. A similar pattern
648 exists in the Grid element view (data not shown). However, note that while the pattern is similar
649 to previous experiments, the numbers of Malignant cells are markedly lower than in Figure 32
650 and Figure 42.

651

PeerJ PrePrints | https://doi.org/10.7287/peerj.preprints.1558v1 | CC-BY 4.0 Open Access | rec: 3 Dec 2015, publ: 3 Dec 2015

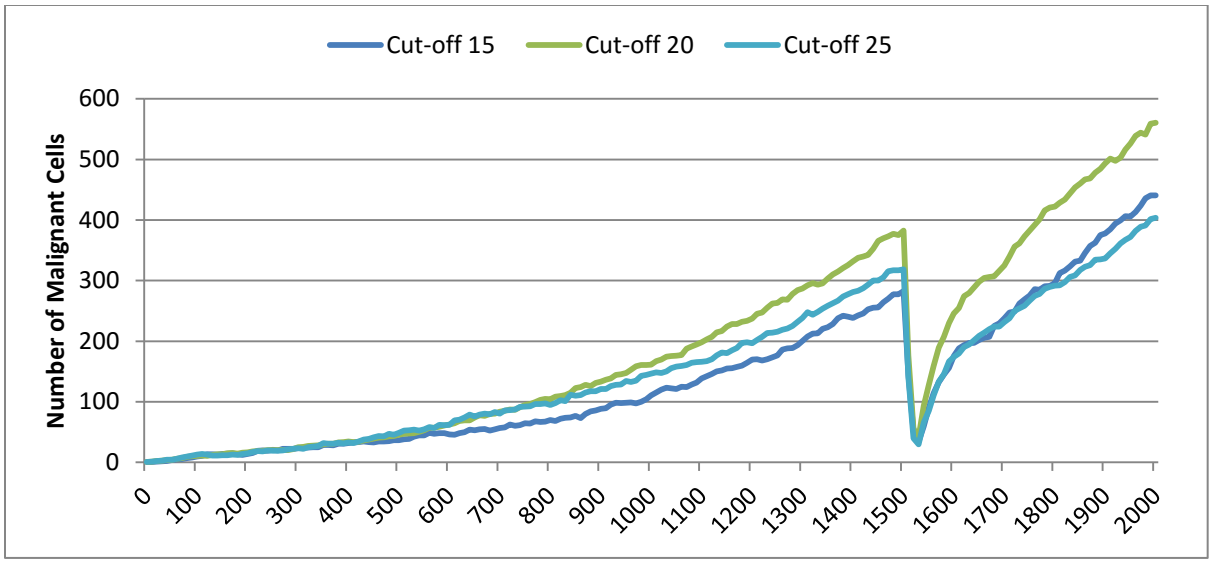

Figure 49 - Malignant cell numbers vs no collateral damage

In terms of the impact on clonal evolution, Figure 50, while there is a pause during the treatment period, it continues at a similar rate to the pre-treatment trend afterwards. Again, while this pattern is familiar, the number of clonal sub-populations is lower than in previous experiments, as shown by Figure 39 and Figure 45.

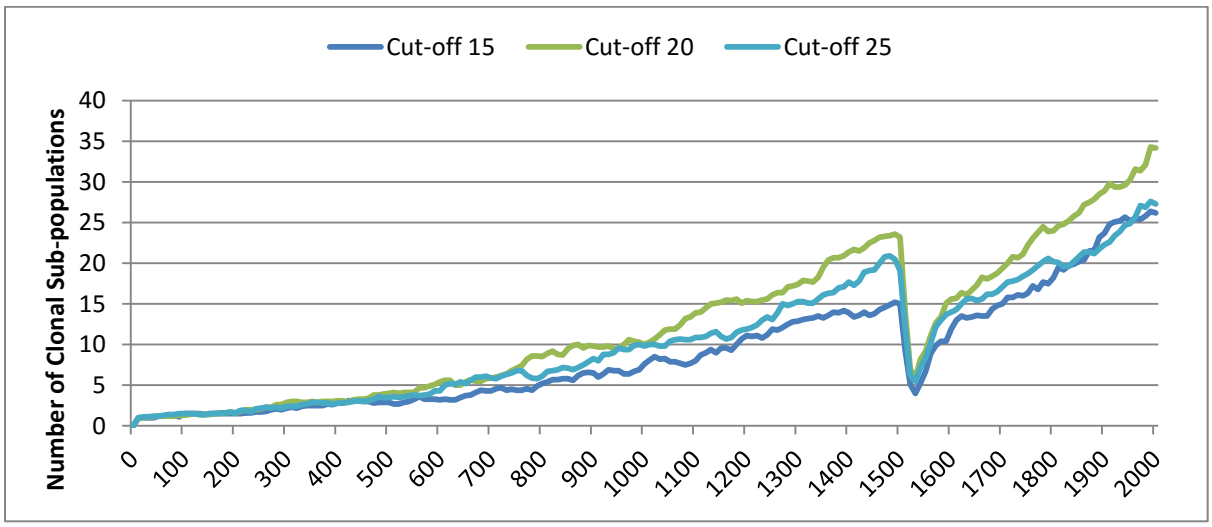

Figure 50 – Clonal Populations vs no collateral damage

Discussion

The NEATG model is not a computational model that attempts to emulate the biological processes involved in tumour growth, indeed it is a very simplistic model that lacks even the bare essentials of tumour physiology. It does not include any modelling of the immune system, it is completely avascular, nor does it model specific cell populations. In some respects it may appear as a simple model of stratified epithelial tissues – the model is partly cellular, the cells are

PeerJ PrePrints | https://doi.org/10.7287/peerj.preprints.1558v1 | CC-BY 4.0 Open Access | rec: 3 Dec 2015, publ: 3 Dec 2015

667 homogeneous and nutrient supply is diffusive rather than via vascular transport – but this is not
668 the intention. Despite the non-physiological basis of the model, however, the results display a
669 range of behaviours and phenomena which are indicative of real tumour growth. In many
670 respects these are emergent behaviours that may be shed light on biologically relevant systems.

671 In the first instance the model is capable of reproducing homeostatic behaviour. In optimal
672 conditions, (i.e. with an ideal supply of Nutrient and Gene Factors), the model displays a steady
673 turnover of cells, which age and divide in such a manner that the target cell population is
674 preserved. However, under conditions of stress, such as a restriction in the Nutrient supply or a
675 reduction in Gene Factors, we see a change in behaviour. In the case of underfeeding or
676 starvation we see that cell numbers are markedly reduced, however over-feeding does not lead to
677 an increase in cell populations.

678 In the case of variations in Gene Factors, we see that under or over-supply of these factors does
679 not impact cell numbers to the same extent, though both scenarios lead to a small reduction in
680 total cell numbers. The variations in Gene Factor supply do however impact on cell turnover,
681 with an increase in rates of cell division in both under and over-supply situations. In this respect
682 we may view the impact of deviations from the Gene Factor target values acting as mitogenic
683 factors. There is also a marked impact on the calculation of cell fitness, with deviations from the
684 optimal values for Gene Factors reducing the fitness value. We may conclude, therefore, that
685 variations in the Gene Factor supply are deleterious to some extent, but do not cause the same
686 level of cellular damage as restriction in the supply of Nutrient.

687 In the case of tumour growth, we see that once initiated the proliferation of cancer cells numbers,
688 and the attendant increase in the number of affected Grid Elements, increases in the absence of
689 any counter-measures (i.e. left untreated). As each Grid Element can support a number of cells
690 over and above the optimum level, this initial increase in numbers does not displace or replace
691 non-cancer cells. However, once the carrying capacity of the Grid Element has been reached
692 there is a competition between cells in which ultimately the Malignant cells out-compete the
693 Normal cells. Over time the number of Malignant cells increases and the rate of invasion
694 increases, while there is a corresponding decrease in Normal cells. As with the homeostatic case,
695 this behaviour is not pre-programmed but emerges from the interactions between the cells,
696 interactions between neighbouring Grid Elements and the operation of a few simple rules.
697 Additionally, there is a consistent increase in the number of clonal sub-populations as growth
698 continues – mirroring the genetic heterogeneity which is a hall-mark of real tumour growth.
699 What is more the system shows that in the face of changing conditions there is an increase in the
700 number of clonal sub-populations and a decrease in the dominance of the most populous sub-
701 clone over time.

702 Of note is the fact that in the first instance the seeded Malignant cell has the same genomic
703 structure as the Normal cell population in these experiments. That is the Malignant cell is not
704 conferred any genetic advantage over the rest of the non-Malignant cell population. The single
705 difference between the Malignant cell and the Normal cell is that the Malignant cell is flagged as
706 such and that it therefore has an ability to mutate, proliferate and undergo repeated division. In
707 terms of Genomic structure, cell Lifetime, nutrient requirements and so on there are no
708 differences initially between cell types. It may be assumed that the increasing success of the
709 Malignant cells in outcompeting Normal cells may be due to an increasing evolutionary fitness

PeerJ PrePrints | https://doi.org/10.7287/peerj.preprints.1558v1 | CC-BY 4.0 Open Access | rec: 3 Dec 2015, publ: 3 Dec 2015

that arises through a succession of mutational events occurring during cell division. However, a simple reading of the data does not support this assumption.

Evolutionary fitness is not defined in absolute or global terms in NEATG. Instead it is a local definition that reflects cellular adaption to the conditions in each Grid Element. Thus it is clear from the data, as shown in Figure 12, that in general the fitness of many Malignant cells is lower than the initial fitness of the Normal cells, and that it often decreases as a result of intra-Grid Element competition between cells. Furthermore, it is clear that many mutations are actually deleterious and do not confer evolutionary advantage over competing cells, Normal or Malignant. Some Malignant cells do experience mutations which provide an advantage, and these are the cells which manage to survive and expand in number. However, a cell with a positive advantage in one Grid Element may migrate to an adjacent Grid Element and find that it is less fit and therefore does not survive. This view of evolutionary fitness as locally responsive to the environment and therefore having an impact on the success, or otherwise, of genetic mutations is in line with more recent theoretical models of evolutionary processes in cancer (Rozhok & DeGregori, 2015).

The rate of evolutionary change is initially set by the Mutation Rate, which is heritable and mutable. It may be thought that the Mutation Rate would be an important driver in the rate of cancer growth, however our data show that in this model it has a weak influence on the rate of growth of cancer – both in terms of Malignant cell numbers and affected Grid Elements. It does however directly influence the size of the Gene Pool and the number of clonal sub-populations.

More influential in terms of driving growth is the Invasion Rate, which represents the probability that a dividing Malignant cell in an over-crowded Grid Element can migrate to a neighbouring Grid Element. The data show that this is a very strong driver of growth rates, but it does not lead to the same increase in the size of the Gene Pool or the number of clonal sub-populations.

In terms of modelling interventions against the tumour growth we have explored the use of a treatment option that loosely mimics maximum tolerated dose chemotherapy in two key respects. Firstly the treatment is not genetically targeted – it applies to both Normal and Malignant cells, though we can confer an increased sensitivity to Malignant cells if required. Secondly the treatment induces cell death in affected cells, analogous to the apoptotic or necrotic cell death induced by chemotherapy. And finally cells are affected depending on where they are in the cell cycle – which is modelled in this instance by the reading of the cell clock.

The response to this treatment, which we have varied in intensity and duration, is consistent in our experiments. There is an initial response marked by massive tumour kill followed by a resumption of tumour growth, which is often characterised by an accelerated and aggressive tumour expansion. This response to treatment bears some resemblance to real cancer treatment, where an initial reduction in tumour growth characterised as complete or partial remission is followed by renewed tumour growth or the appearance of metastatic disease. While the mechanisms of treatment resistance in real tumours is complex and multifactorial it is assumed that tumour heterogeneity is an important factor; a tumour may harbour clonal subpopulations which are resistant to treatment and which therefore benefit from reduced competition after chemo-sensitive populations have been destroyed by treatment. In the NEATG model treatment resistance is not related to drug efflux or other mechanisms of acquired resistance. Instead the phenomenon is associated with a pool of cells which survive due to their age (i.e. they are above

PeerJ PrePrints | https://doi.org/10.7287/peerj.preprints.1558v1 | CC-BY 4.0 Open Access | rec: 3 Dec 2015, publ: 3 Dec 2015

753 the treatment cut-off age) and which are therefore faced with a decreased level of competition for
754 resources and a lower population density of cells in each Grid Element.

755 Increasing the intensity or duration of treatment as a strategy to improve response is shown to be
756 problematic in that it can cause reductions in Normal cell numbers which do not recover and
757 therefore this strategy is assumed to be deleterious. Again, there is a clear parallel to clinical
758 experience in which increased toxicity causes excess morbidity without necessarily leading to
759 improved outcomes.

760 While the NEATG model displays emergent behaviour that corresponds with clinical
761 phenomena, the question that arises is whether there is anything that we can learn from such a
762 system. Can a non-physiological model shed any new light on real biological systems? Clearly
763 drawing conclusions at a molecular or genetic level is out of the question, but there are
764 algorithmic features of biological systems that may be amenable to exploration using software
765 models such as this one.

766 For example, at a very fundamental level there remain competing views on the nature and origin
767 of the cancerous state. At a simplistic level the SMT places the delinquent cell at the centre of
768 cancer development, whereas the TOFT places the poor neighbourhood central to the story
769 (Baker, 2014; Sonnenschein et al., 2014). A central difference between these competing theories
770 is in the role of cellular proliferation. The SMT suggests that in the non-transformed state cells
771 are non-proliferative by default. Mutations in genes associated with cell cycle control mean cells
772 become proliferative and malignant. In contrast the TOFT posits that cells are proliferative by
773 default and that this proliferative ability is kept in check at the tissue level. A disordered tissue
774 results in the removal of the proliferative blocks and the cell can multiply without control.

775 In our model both cell and tissue (Grid Element) level structures are featured. The process of
776 cancer initiation consists of seeding a transformed cell into a grid element and letting it
777 proliferate. The model does not have anything to say about how the initial cell is transformed, it
778 is taken as a given. The initial cell has the same parameters as the untransformed cells, the only
779 difference is that proliferative blocks have been removed. The transformed cell, and its progeny,
780 is able to accumulate mutations during cell division and replication. Some of these mutations
781 will be deleterious and some will be advantageous, we would expect therefore that the average
782 fitness of the Malignant population will increase and that these advantageous mutations will
783 drive further evolutionary change – particularly mutations that increase the Invasion rate.
784 However this does not appear to occur. Indeed, a surprising result is that neither the Mutation
785 Rate nor the Invasion Rate, which are both heritable and mutable, appear to undergo significant
786 increase during the process of tumour growth. In fact, as shown in Figure 14, both show
787 marginal rates of change, and can rise and fall rather than rising monotonically and driving
788 malignant growth. While some mutations may provide evolutionary advantage, it is clear that the
789 majority of mutations are passenger mutations rather than driver mutations. This is another
790 instance where the NEATG model parallels biological systems, as it has become increasingly
791 clear that the majority of somatic mutations in human tumours are also passenger mutations,
792 many of which are actively deleterious to the cancer cell (Greenman et al., 2007; McFarland et
793 al., 2013; McFarland, Mirny & Korolev, 2014).

794 The question arises then as to whether mutational change is a necessary precondition for cancer
795 growth in this model. To investigate this question an additional series of experiments was

PeerJ PrePrints | https://doi.org/10.7287/peerj.preprints.1558v1 | CC-BY 4.0 Open Access | rec: 3 Dec 2015, publ: 3 Dec 2015

performed in which the Mutation Rate was set at zero, and the Invasion Rate varied from zero to 8% in increments of 2%, with all other settings as in the previous set of experiments. The results show that Malignant cell growth can occur even with a zero Mutation rate, which was verified by confirming that the Gene Pool retained a constant value of 1. The rate of growth, as shown in Figure 51, depends on the Invasion Rate, as one would expect, but that even at the lowest non-zero rate tumour growth occurs, and furthermore the growth rate accelerates after treatment.

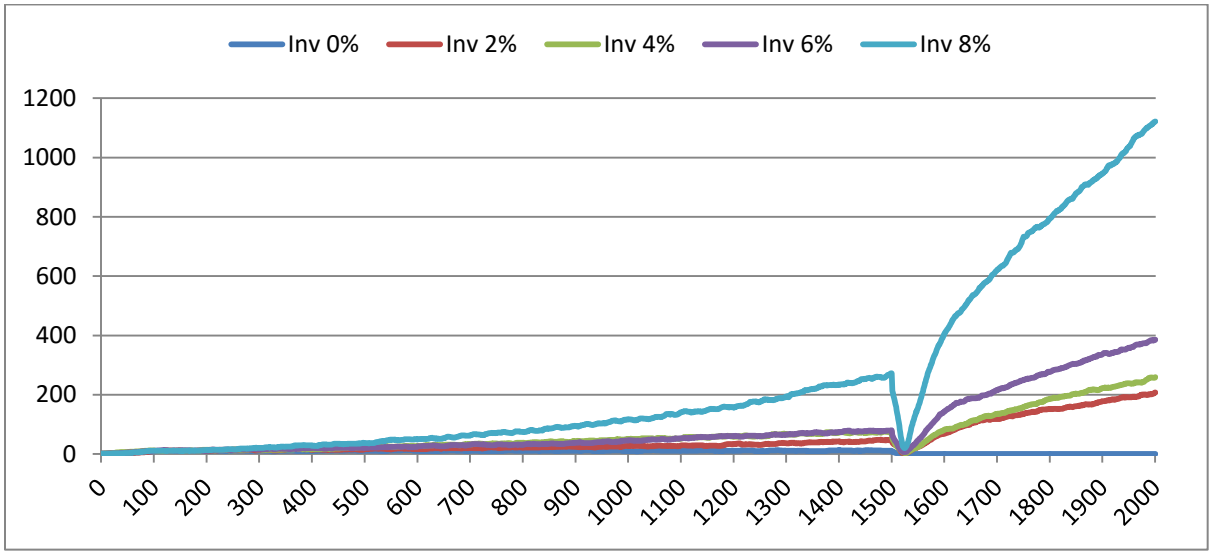

Figure 51 - Malignant Cells with Zero Mutation Rate vs Changing Invasion Rate

What is more, the data shows that with a zero rate of Invasion and Mutation there is growth in Malignant cell numbers to the maximum possible in the Grid Element where seeding occurred, but that without an Invasion Rate there is no possibility of a Malignant cell migrating to a neighbouring Grid Element. One implication of this result is that in the NEATG model cancer growth is not driven primarily by somatic mutation and is primarily dependent on proliferation and invasiveness. This is closer to the tissue organisation field theory view of cancer development than the somatic mutation theory view.

Clearly this is a very simple model that does not incorporate many biologically relevant oncogenic mechanisms. In particular it may be argued that even within its own terms this model is perhaps too simplistic in the handling of genetic change. While the model reproduces the evolution of clonal sub-populations and an increased Gene Pool, it can be argued that scope for evolution of advantageous traits is limited. The model does not include the possibility that chance mutation can switch on pre-existing pathways and signalling networks which are common in real cancers, for example pathways that enable metabolic adaptations to nutrient stress, hypoxia, angiogenesis and so on. It might also be argued that the fundamental difference between Normal and Malignant cells in this model, which is simply the ability to proliferate and invade, is of such fundamental importance and represents such a significance difference between cellular phenotypes that a model which simply assigns this as a given does not have any real world validity.

Another area where the model may benefit from further development is in the handling of Gene Factors. There is scope for the modelling of more complex feedback loops between the genes

PeerJ PrePrints | https://doi.org/10.7287/peerj.preprints.1558v1 | CC-BY 4.0 Open Access | rec: 3 Dec 2015, publ: 3 Dec 2015

and the environment, perhaps including some aspects of oncogene addiction (Luo, Solimini & Elledge, 2009). Addressing this issue may also address the concern that the model does not provide sufficient scope for the discovery of advantageous driver mutations.

NEATG is designed as an extendable platform for investigating different interventions and how they impact the growth of Malignant cells and the spread of affected Grid Elements. In the experiments described in this paper only one intervention, loosely based on maximum tolerated dose chemotherapy, has been explored. Clearly there is scope for additional interventions to be modelled, for example combinations of Nutrient restriction and chemotherapy, a treatment strategy of some clinical interest (Raffaghello et al., 2008; Safdie et al., 2009; Lee et al., 2012), may be modelled in NEATG. Similarly the use of metronomic chemotherapy, targeted therapies and the use of different treatment schedules are also amenable to modelling using the NEATG system.

Conclusion

The value of agent-based evolutionary models is that they can generate biologically relevant behaviour through algorithmic means, which may in turn shed light on how these are implemented in biological systems. Obviously increasing the complexity of the model so that additional features are included, for example an improved mechanism for modelling advantageous genetic changes, may be of some value. However, in another sense retaining a simple model may be provide greater insight into the abstract processes involved in reproducing cancer-like behaviour – perhaps casting light on the disputed territory between the somatic mutation and tissue organisation field theories.

PeerJ PrePrints | https://doi.org/10.7287/peerj.preprints.1558v1 | CC-BY 4.0 Open Access | rec: 3 Dec 2015, publ: 3 Dec 2015

References

Allen M., Louise Jones J. 2011. Jekyll and Hyde: the role of the microenvironment on the progression of cancer. *The Journal of pathology* 223:162–76.

Baker SG. 2014. A Cancer Theory Kerfuffle Can Lead to New Lines of Research. *JNCI Journal of the National Cancer Institute* 107:dju405–dju405.

Barcellos-Hoff MH., Lyden D., Wang TC. 2013. The evolution of the cancer niche during multistage carcinogenesis. *Nature reviews. Cancer* 13:511–8.

Basanta D., Simon M., Hatzikirou H., Deutsch a. 2008. Evolutionary game theory elucidates the role of glycolysis in glioma progression and invasion. *Cell Proliferation* 41:980–987.

Bizzarri M., Cucina A. 2014. Tumor and the microenvironment: a chance to reframe the paradigm of carcinogenesis? *BioMed research international* 2014:934038.

Fisher R., Pusztai L., Swanton C. 2013. Cancer heterogeneity: implications for targeted therapeutics. *British journal of cancer* 108:479–85.

Gatenby RA., Gillies RJ., Brown JS. 2011. Of cancer and cave fish. *Nature reviews. Cancer* 11:237–238.

Gerlee P., Basanta D., Anderson ARA. 2011. Evolving homeostatic tissue using genetic algorithms. *Progress in Biophysics and Molecular Biology* 106:414–425.

Gillies RJ., Verduzco D., Gatenby R a. 2012. Evolutionary dynamics of carcinogenesis and why targeted therapy does not work. *Nature reviews. Cancer* 12:487–493.

Greenman C., Stephens P., Smith R., Dalgliesh GL., Hunter C., Bignell G., Davies H., Teague J., Butler A., Stevens C., Edkins S., O'Meara S., Vastrik I., Schmidt EE., Avis T., Barthorpe S., Bhamra G., Buck G., Choudhury B., Clements J., Cole J., Dicks E., Forbes S., Gray K., Halliday K., Harrison R., Hills K., Hinton J., Jenkinson A., Jones D., Menzies A., Mironenko T., Perry J., Raine K., Richardson D., Shepherd R., Small A., Tofts C., Varian J., Webb T., West S., Widaa S., Yates A., Cahill DP., Louis DN., Goldstraw P., Nicholson AG., Brasseur F., Looijenga L., Weber BL., Chiew Y-E., DeFazio A., Greaves MF., Green AR., Campbell P., Birney E., Easton DF., Chenevix-Trench G., Tan M-H., Khoo SK., Teh BT., Yuen ST., Leung SY., Wooster R., Futreal PA., Stratton MR. 2007. Patterns of somatic mutation in human cancer genomes. *Nature* 446:153–158.

Hanahan D., Coussens LM. 2012. Accessories to the Crime: Functions of Cells Recruited to the Tumor Microenvironment. *Cancer Cell* 21:309–322.

Janes K a., Lauffenburger D a. 2013. Models of signalling networks - what cell biologists can gain from them and give to them. *Journal of cell science* 126:1913–21.

Kareva I. 2011. What can ecology teach us about cancer? *Translational oncology* 4:266–70.

Krzeslak M., Swierniak A. 2014. Four Phenotype Model of Interaction Between Tumour Cells. In: *World Congress*. 11536–11541.

Lee C., Raffaghello L., Brandhorst S., Safdie FM., Bianchi G., Martin-Montalvo A., Pistoia V., Wei M., Hwang S., Merlino A., Emionite L., de Cabo R., Longo VD. 2012. Fasting cycles retard growth of tumors and sensitize a range of cancer cell types to chemotherapy. *Science translational medicine* 4:124ra27.

Luo J., Solimini NL., Elledge SJ. 2009. Principles of Cancer Therapy: Oncogene and Non-oncogene Addiction. *Cell* 136:823–837.

PeerJ PrePrints | https://doi.org/10.7287/peerj.preprints.1558v1 | CC-BY 4.0 Open Access | rec: 3 Dec 2015, publ: 3 Dec 2015

McFarland CD., Korolev KS., Kryukov G V., Sunyaev SR., Mirny L a. 2013. Impact of deleterious passenger mutations on cancer progression. *Proceedings of the National Academy of Sciences* 110:2910–2915.

McFarland CD., Mirny LA., Korolev KS. 2014. Tug-of-war between driver and passenger mutations in cancer and other adaptive processes. *Proceedings of the National Academy of Sciences* 111:15138–15143.

Pantziarka P. 2015. Primed for cancer: Li Fraumeni Syndrome and the pre-cancerous niche. *Ecancermedicalscience* 9:541.

Psaila B., Kaplan RN., Port ER., Lyden D. 2007. Priming the “soil” for breast cancer metastasis: the pre-metastatic niche. *Breast disease* 26:65–74.

Quail DF., Joyce J a. 2013. Microenvironmental regulation of tumor progression and metastasis. *Nature medicine* 19:1423–37.

Raffaghello L., Lee C., Safdie FM., Wei M., Madia F., Bianchi G., Longo VD. 2008. Starvation-dependent differential stress resistance protects normal but not cancer cells against high-dose chemotherapy. *Proceedings of the National Academy of Sciences of the United States of America* 105:8215–20.

Rozhok AI., DeGregori J. 2015. Toward an evolutionary model of cancer: Considering the mechanisms that govern the fate of somatic mutations. *Proceedings of the National Academy of Sciences of the United States of America* 112:8914–8921.

Saetzler K., Sonnenschein C., Soto AM. 2011. Systems biology beyond networks: Generating order from disorder through self-organization. *Seminars in Cancer Biology* 21:165–174.

Safdie FM., Dorff T., Quinn D., Fontana L., Wei M., Lee C., Cohen P., Longo VD. 2009. Fasting and cancer treatment in humans: A case series report. *Aging* 1:988–1007.

Silva AS., Gatenby R a. 2010. A theoretical quantitative model for evolution of cancer chemotherapy resistance. *Biology direct* 5:25.

Sonnenschein C., Soto AM., Rangarajan A., Kulkarni P. 2014. Competing views on cancer. *Journal of biosciences* 39:281–302.

De Sousa E Melo F., Vermeulen L., Fessler E., Medema JP. 2013. Cancer heterogeneity--a multifaceted view. *EMBO reports* 14:686–95.

Tian T., Olson S., Whitacre JM., Harding A. 2011. The origins of cancer robustness and evolvability. *Integrative biology : quantitative biosciences from nano to macro* 3:17–30.

PeerJ PrePrints | https://doi.org/10.7287/peerj.preprints.1558v1 | CC-BY 4.0 Open Access | rec: 3 Dec 2015, publ: 3 Dec 2015